International
WOCE
Newsletter

Number 40 ISSN 1029-1725 December 2000

IN THIS ISSUE

News from the WOCE IPO

W. John Gould, Director, WOCE IPO and ICPO, Southampton Oceanography Centre, UK. john.gould@soc.soton.ac.uk

The postal services of the world seem to have a remarkable skill in delivering poorly addressed items. We recently received a letter addressed to us at SOC, Express Duck, Southampton. In the past we have also had a letter to the WOE IPO. The latter seems rather apt at the moment because WOCE is about to lose the services of two key people involved in its running.

Farewell Bert and Roberta

Bert Thompson from the Data Information Unit in the University of Delaware has worked tirelessly in recent years to iron out inconsistencies in the information we have on the various WOCE data sets. He will be best known to most of you as the person who (usually at meetings when you can't escape) asks searching questions about exactly when and where your observations were made. Our comprehensive summary of WOCE observations will owe a great deal to Bert's persistence and attention to detail. Bert has been involved with WOCE from the very beginning since his time at IOC during the formative years of the project and then in the IPO in the late 1980s as the Implementation Plan was being constructed and the first observations started.

In some senses Bert has worked himself out of a job in WOCE and instead will continue to work part-time in Delaware on similar tasks for the Global Ocean Observing System.

About WOCE

The World Ocean Circulation Experiment (WOCE) is a component of the World Climate Research Programme (WCRP), which was established by WMO and ICSU, and is carried out in association with IOC and SCOR.

WOCE is an unprecedented effort by scientists from more than 30 nations to study the large-scale circulation of the ocean. In addition to global observations furnished by satellites, conventional in-situ physical and chemical observations have been made in order to obtain a basic description of the physical properties and circulation of the global ocean during a limited period.

The field phase of the project lasted from 1990–1997 and is now being followed by Analysis, Interpretation, Modelling and Synthesis activities. This, the AIMS phase of WOCE, will continue to the year 2002.

The information gathered during WOCE will provide the data necessary to make major improvements in the accuracy of numerical models of ocean circulation. As these models improve, they will enhance coupled models of the ocean/atmosphere circulation to better simulate – and perhaps ultimately predict – how the ocean and the atmosphere together cause global climate change over long periods.

WOCE is supporting regional experiments, the knowledge from which should improve circulation models, and it is exploring design criteria for long-term ocean observing system.

The scientific planning and development of WOCE is under the guidance of the Scientific Steering Group for WOCE, assisted by the WOCE International Project Office (WOCE IPO):

- W. John Gould, *Director*
- Peter M. Saunders, *Staff Scientist*
- N. Penny Holliday, *Project Scientist*
- Roberta Boscolo, *Project Scientist*
- Sheelagh Collyer, *Publication Assistant*
- Jean C. Haynes, *Administrative Assistant*

For more information please visit:
http://www.soc.soton.ac.uk/OTHERS/woceipo/ipo.html

This Newsletter will be the last to be edited by Roberta Boscolo. If you look back through the issues you will see how the Newsletter has evolved from a rather thin and irregular publication containing news of meetings to what you see today, a very professional and regular means of communication that puts many refereed journals in the shade. Roberta's influence has been strong. She has been persuasive in getting authors to contribute articles and then unrelenting in ensuring that the contents, and particularly the figures, were of a high standard. Her contribution has not been confined to the Newsletter. High-quality visual material is very important in giving professional presentations and WOCE's image has benefited immensely from Roberta's Italian eye for colour and layout.

Roberta is moving to Vigo in northern Spain where she will start a 2 year fellowship working on the variability of oceanographic conditions west of the Iberian peninsula. We wish her all the best for the future. She will not be totally disconnected from WCRP as she will continue to provide support for CLIVAR's Atlantic sector panel. Her impact on the WOCE IPO has been enormous. We will miss her contribution to the Office but most of all we will miss her as a colleague and a friend.

But life goes on

Despite these staff departures WOCE activities continue unabated. Not least of these is the SSG's decision at its meeting in Fukuoka in October to continue with the WOCE Newsletter. For this a new editor must be found, so if anyone is interested…

The SSG followed the WOCE Workshop on Variability and Representativeness that is reported on page 27. I want to thank Terry Joyce and Shiro Imawaki for the excellent job they did in organising the meeting and particularly for Shiro and his colleagues for being such excellent hosts and for obtaining such a generous level of financial support.

At the SSG some decisions were made about a Conference to mark the formal end of WOCE as a part of WCRP in 2002. The Conference will be held in San Antonio, Texas late in 2002. Carl Wunsch and Worth Nowlin have agreed to co-chair the organising committee that is now almost ready to start work.

We have now secured the funding from BP-Amoco for the production of hard copy WOCE Atlases and a meeting of the PIs concerned is being planned for early in 2001 to set the scene for the production of the first (Pacific) Atlas.

We at the WOCE IPO send you good wishes for 2001.

Ocean Circulation and Climate.
Observing and modelling the global ocean

Eds. Gerold Siedler, John Church and John Gould ca 900pp.

Published by Academic Press. $100.

The book is in the final stages of preparation and should be launched at the EGS in Nice in late March 2001. A "flyer" is enclosed with this issue of the Newsletter. People who attended the WOCE Conference in Halifax in 1998 will be entitled to a 20% discount on the purchase price. They will be contacted by the WOCE IPO early in the New Year and invited to place an order.

Subinertial variability of transport estimates across "48°N" in the North Atlantic

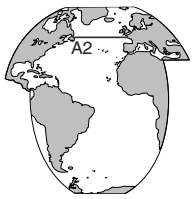

Katja Lorbacher and Klaus-Peter Koltermann, Bundesamt für Seeschiffahrt und Hydrographie, Hamburg, Germany. lorbacher@bsh.d400.de

The estimation of advective oceanic transports of mass (volume), heat and freshwater was one of the main challenges within the WOCE hydrographic programme. Temporal changes in these integral parameters manifest both changes in the large-scale ocean circulation and changes in the properties of the advected water masses. Thus they are directly linked to climate variations on regional and global scales. Using the hydrographic data from seven realisations of the so-called "48°N"-section between the English Channel and the Grand Banks off Newfoundland the subinertial, climate relevant variability of the large-scale ocean circulation in the northern North Atlantic and its integral key parameters were determined for the first time from observations alone.

The data consist of five available sets of the WOCE A2 section during the Nineties for the years 1993, 1994, 1996, 1997, 1998 and of two previous transatlantic cruises in April 1957 and 1982. The realisations of the WOCE A2 section were carried out in the same season (May to July), except for the cruise in October 1994. In addition, we consider also two recent realisations of the WOCE A2 section in October 1999 and May 2000, where the results are still preliminary. The "48°N"-section follows the divergence zone of the mainly wind-driven subtropical gyre and the more complex, with respect to the forcing, subpolar gyre. This is marked by the line of zero wind stress curl $(\mathrm{curl}_z \vec{\tau})$ - the zone of westerlies of the North Atlantic. In the central West European and Newfoundland Basins the section runs a few degrees south of the line of zero $\mathrm{curl}_z \vec{\tau}$. In the West, the WOCE A2 section turns northwest to cross the boundary current regime perpendicularly. Therefore this quasi-zonal hydrographic section covers all large-scale circulation elements on the regional scale that contribute essentially to the ocean circulation on the global scale – the Meridional Overturning Circulation (MOC) – the projection of the three-dimensional circulation on the meridional-vertical plane.

Method and results

The transport estimates are given as the sum of the three transport components of a quasi-stationary, large-scale ocean circulation (Jung, 1952; Bryan, 1962; Hall and Bryden, 1982): the ageostrophic Ekman-, and the two geostrophic components, the depth-independent, barotropic or Sverdrup- and the baroclinic component, which reflects the measured vertical shear due to the zonal density gradient. The compensation of each component is assumed to maintain both the mass balance over the plane of the section (the advection of potential temperature can be defined as heat transport (Montgomery, 1974; Warren, 1999)) and to resolve the transport profile as a function of depth (Dobroliubov et al., 1996, Koltermann et al., 1999). In the case of the baroclinic component the balance is achieved through a suitable choice for a surface of "no-motion". The absolute meridional velocity as a function of the zonal distance along the section and depth is therefore the sum of the three components and their compensatory components, respectively, at each point of the area integral of the mass transport (details in Lorbacher, 2000).

The transport estimates should be representative for the particular year. To minimise the seasonal variability of the baroclinic component most of the WOCE-cruises took place in the same season. Under the assumption that the vertically-integrated Sverdrup-relation yields the depth-independent part of the geostrophic current in the ocean interior the Sverdrup-component is derived from the Sverdrup-balance (Wunsch and Roemmich, 1985; Pedlosky, 1996). So far only one measurement of the depth-independent part at "48°N" is available (Meinen, 1998). However, the seasonal variability of the two wind-driven parts is larger than both the annual and interannual. Thus the Ekman- and Sverdrup-components are estimated from long-term monthly means of wind data from the NCEP/NCAR reanalysis project (Kalnay et al., 1996).

On interannual scales the largest change in the meridional overturning rate – the volume transport of the upper limb of the MOC, the one above the reference level – is observed between May 1996 and June 1997 (Fig. 1, page 15). The amount decreases from a maximum of 21 Sv to a minimum of 13 Sv only one year later, defining a range of 8 Sv. On decadal time scales the overturning rate shows roughly the same range but with an inverse sign: the rate increases from 13 Sv in 1957 to 20 Sv in 1982. Therefore the rates of the years 1957 and 1982 (with a reduced spatial resolution and a different cruise track, respectively (Fig. 1)) correspond well with the ones derived from the consistent data sets during the nineties. The transport of the water masses below the reference level shows the largest variation during the WOCE-period (1990–1998) between 1993 and 1994 (Fig. 1). Between these years, also the largest changes in the thermohaline structure is observed and therefore these changes seem not to reflect methodical uncertainties (Lorbacher, 2000). The upper component of the deep water represents the major part of the total deep water transport, whilst the lower component, the DSOW, is the dominant contributor to variations in the deep transport. At decadal time scales the variable vertical gradient between the LSW and deep water transports due to the changes in the DSOW transport is decisive for the shift between two modes of the

vertical profile of the MOC (Koltermann et al., 1999).

The transports of heat and freshwater show a similar temporal evolution like the overturning rate with the exception of the changes in the southward freshwater transport between 1993 and 1994 having opposite sign (Fig. 2, page 15). Changes in the overturning rate explain 85% of changes in the heat transport and 55% of in the freshwater transport (not shown). The observed temporal variability of the meridional overturning rate vary at 16.1 Sv by ±20%, in the heat transport at 0.52 PW by ±30% and in the southward freshwater transport at 0.98 Sv by ±20%. Generally, our absolute transports – assuming that the Sverdrup-balance delivers the depth-independent transport part – correspond well with values recently derived with the inverse method (Ganachaud, 1999; Woelk, 2000).

The largest methodical uncertainties explain only 50% of the temporal changes in the meridional overturning rate and the heat transport, due to the seasonal variability of the Ekman-component and to the depth-independent part, which is not derived from the wind field. For the freshwater transport they match only 5% of the temporal variability (Lorbacher, 2000). The baroclinic part of the transports, the change in the mechanical energy is mainly responsible for the observed temporal changes. Tidal forces and fluctuations in the wind field are the main sources of mechanical energy to force advection and mixing in ocean interior (Munk and Wunsch, 1998). The NAO-index quantifies fluctuations of the wind field over the North Atlantic – positive values stand for strong westerlies and maritime climate conditions over Northern Europe and the east coast of North America (Hurrell, 1995).

The particular transport types during the WOCE-period exhibit a short-term variability that appears to be a close reflection of the extreme interannual behaviour of the NAO-index since 1993. The heat transport for example drops from 0.70 PW in 1996 to 0.30 PW just one year later, following the decline of the NAO-index between winter 1995 and winter 1996, and recovers equally rapidly to 0.60 PW in summer 1998 when the NAO-index returns to positive values (Fig. 2). The two estimates of the heat transport in 1957 and 1982 are not inconsistent with this behaviour of a fast oceanic response to atmospheric fluctuations. The observed temporal changes in the heat transport seem to reflect changes in the NAO-index with a time-lag of about one year. For this phase lag the changes in the NAO-index explain 70% of the changes in heat and 65% in freshwater transports as well as 60% in the meridional overturning rate (Fig. 3). Though based on only few occupations, this dramatic behaviour may be a first indication that short-term changes in atmospheric forcing, however extreme, may be matched by an equally rapid response in the large-scale ocean circulation. The "dynamical response" is most pronounced at a location east of the western boundary current regime for the WOCE-period (not shown). After the almost linear correlation of changes in the NAO-index and the transport variability one would expect a heat transport around 0.60 PW for the year 2000 after a high positive NAO-index for the last two years. But now we observe transport minima with the main signal coming from the western boundary area – coinciding strong eastward penetration of the cold Labrador Current and a reduced warm core of the North Atlantic current (NAC). For the whole data set the explained variance between changes in the NAO-index and transports is reduced to 30%, 40% and 15%, respectively (Fig. 3).

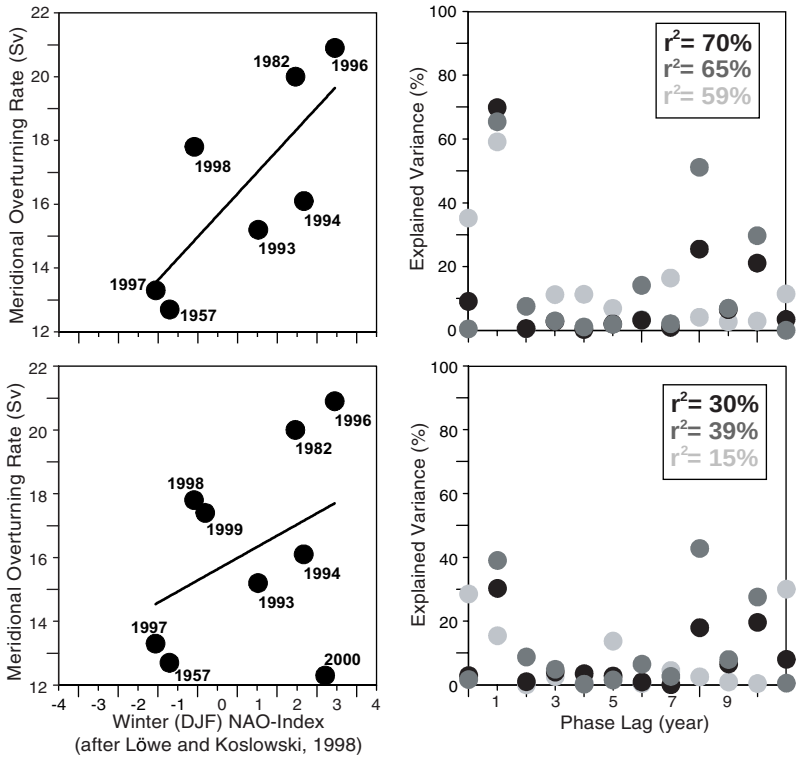

Figure 3. Correlation between the NAO-index and transports for a phase lag of one year and explained variance of this correlation for different phase lags (upper: Δt: 1957–1998, lower: Δt: 1957–2000).

The baroclinic transport is mainly responsible for the observed changes. It contributes more than 80% to the total heat transport across the "48°N"-section (Fig. 4). The Sverdrup-transport is nearly negligible at the location of the section, which follows closely the line of zero $\mathrm{curl}_z \vec{\tau}$. After Hall and Bryden (1982) the baroclinic heat transport breaks down into the transport due to the meridional overturning cell with 80% and the eddy-transport with 20% (Fig. 4). This mesoscale variability is independent of the choice of the reference level and seems dynamically relevant to the large-scale ocean circulation at "48°N" in the North Atlantic. Especially the sign of the eddy-component seems to be responsible for the observed changes in the baroclinic

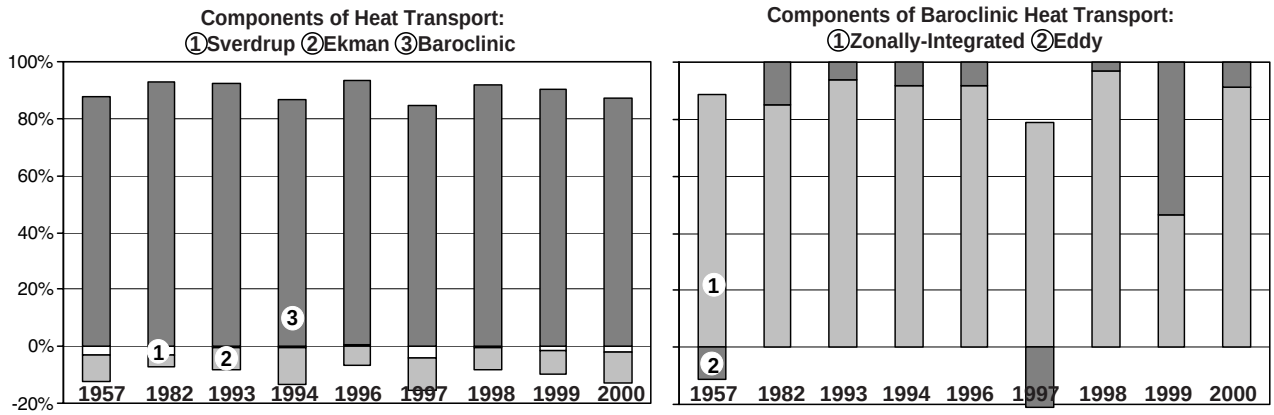

Figure 4. Components of the total meridional heat transport across "48°N" in the North Atlantic.

structure and therefore in the total heat transport. But are the minimum values in 1957 and 1997 really coupled with the negative eddy-component? For the transport minimum observed in 2000 eddy-component is positive.

Not only variations in the intensity of the wind field can force subinertial variability in the oceanic flow field but also shifts in the line of zero $\mathrm{curl}_z \vec{\tau}$. The position of the line in the North Atlantic shifts also with changes in the NAO-index (Fig. 2). For the last thirty years, the line shifts northward over the whole North Atlantic during a period of positive NAO-index. Since 1997 only in the Newfoundland Basin the line shifts northward, whilst in the West European Basin it remains fixed at its southernmost position (Fig. 2). Such shift produces primarily a deformation and/or an acceleration of the subpolar gyre, with a generation of meanders of the NAC, baroclinic instabilities or Rossby wave interaction with the mean current, ultimately mesoscale hydrographic variability. Still up for discussion is which of these mechanisms contribute to the observed temporal transport changes along "48°N" in the North Atlantic and if the changes are possibly a superposition of mesoscale variability due to a decadal trend reflected in the vertical structure of the MOC.

Acknowledgements

This work was supported by the German Federal Ministry of Education and Research BMBF under grant 03F0157B (WOCE) and 03F0246G (CLIVAR). Field work was supported for RV Meteor by Deutsche Forschungsgesellschaft DFG and for RV Gauss by BSH. This support and the cooperation within the WOCE community is gratefully acknowledged.

References

Bryan, K., 1962: Measurements of meridional heat transport by ocean currents. J. Geophys. Res., 67, 3403–3414.

Dobroliubov, S. A., V. P. Tereschenkov and A. V. Sokov, 1996: Mass and heat fluxes at 36°N in the North Atlantic: Comparison of 1993, 1981 and 1959 Hydrographic Surveys. Int. WOCE Newsl., 22, 34–37.

Ganachaud, A., 1999: The error budget of inverse box models. PhD thesis, Massachusetts Institute of Technology.

Hall, M. M., and H. L. Bryden, 1982: Direct estimates and mechanisms of ocean heat transport. Deep-Sea Res., 29, 33–359.

Hurrell, J. W., 1995: Decadal trends in the North Atlantic Circulation: Regional temperatures and precipitation. Science, 269, 676–679.

Jung, G. H., 1952: Note on the Meridional Transport of Energy by the Oceans. J. Mar. Res., 11, 139–146.

Kalnay et al., 1996: The NCEP/NCAR 40-Year Reanalysis Project. Bull. Am. Meteorol. Soc., 77, 437–471.

Koltermann, K. P., A. V. Sokov, V. P. Tereschenkov, S. A. Dobroliubov, K. Lorbacher, and A. Sy, 1999: Decadal changes in the Thermohaline Circulation of the North Atlantic. Deep-Sea Res., Part II, 46, 109–138.

Lorbacher, K., 2000: Niederfrequente Variablität meridionaler Transporte in der Divergenzzone des nordatlantischen Subtropen- und Subpolarwirbels - Der WOCE-Schnitt A2, Berichte des BSH, No. 22, 156pp.

Löwe, P., and G. Koslowski, 1998: The western Baltic sea ice season in terms of mass-related severity index 1879–1992: Spectral characteristics and associations with the NAO, QBO, and solar cycle. Tellus, 50A, 219–241.

Meinen, C. S., 1998: Transport of the North Atlantic Current. PhD thesis, University of Rhode Island.

Montgomery, R. B., 1974: Comments on 'Seasonal Variability of the Florida Current', by Niiler and Richardson. J. Mar. Res., 32, 533–535.

Munk, W. H., and C. Wunsch, 1998: Abyssal recipes II: energetics of tidal and wind mixing. Deep-Sea Res., 45(I), 1977–2010.

Pedlosky, J., 1996: Physics of the Ocean. Springer, New York, 2edn., 453pp.

Warren, B. A., 1999: Approximating the energy transport across oceanic sections, J. Geophys.Res., 104(C5), 7915–7919.

Wunsch, C., and D. Roemmich, 1985: Is the North Atlantic in Sverdrup Balance? J. Phys.Oceanogr., 15, 1876–1880.

Woelk, S., 2000: Über Transporte und Flüsse im nördlichen Nordatlantik im Herbst 1994. PhD thesis, Universität Hamburg.

Decadal differences in the Indian Ocean WOCE I3 section: Water mass changes from the 1960s to 1995

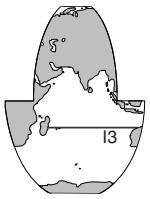

Sarah F. Howe, IASOS, University of Tasmania, Australia, and Nathaniel L. Bindoff, Antarctic CRC, Australia. showe@minke.antcrc.utas.edu.au

The WOCE World Hydrographic Programme (WHP) was designed primarily to describe the state of the global thermohaline circulation during the 1990s and the transports of heat and freshwater. However, the WHP has also given the oceanographic community a unique opportunity to compare these new data with the deep profile data that was collected from 1950 to 1975 for evidence of changes in water masses and circulation. These comparisons are important for validating climate models of natural and anthropogenic climate change. Here we report on a comparison between the WOCE I3 section at 20°S in the Indian Ocean and the available high quality historical data. This report builds on similar comparisons of WOCE hydrographic sections in the Indian Ocean at 32°S (Bindoff and McDougall, 2000) and in the Pacific Ocean (Wong et al., 1999; 2001).

The data and interpolation methods

The WOCE I3 section was obtained in late April to early June 1995. This zonal section, comprising 131 CTD casts, was made along a nominal latitude of 20°S (WOCE CD-ROM, 1998). The historical data set used was that compiled by Reid and Mantyla (pers. comm.) over many years and from many cruises. For comparison with the WOCE I3 section a total of 357 historical casts from the Reid data were taken 10° on either side of this section (Fig. 1). The historical data were collected mostly in the late 1960s, with a standard deviation of about 8 years. The mean year of these data is 1970, and the median date is 1965. Thus, the time interval for this comparison is approximately 25 ±8 years. The most common month in the historical data is July which is two months later in the annual cycle than the WOCE section.

All of the profile data were interpolated to neutral density surfaces (Jackett and McDougall, 1997). A total of 117 unevenly spaced density surfaces were chosen from 22.5 to 28.27 γ_n (kgm^{-3}). Historical salinity, temperature and pressure data were mapped using objective methods to the coordinates of the WOCE hydrographic section. The mapping was done in two stages. For the first stage, long horizontal length scales of 40° (latitude) and 60° (longitude) were used to estimate the long wavelength hydrographic field. For the second stage, the residuals from the first stage were mapped with short length scales of 5° (latitude) and 10° (longitude). The mapped field on the WOCE I3 section consists of the combined short and long wavelength fields from the two mapping stages.

The a priori noise (Fig. 2) was estimated from the standard deviation of the difference between close neighbouring profiles. The method used here is the same as in Bindoff and McDougall (2000) and Bindoff and Wunsch (1992) and this noise estimate represents the contribution of seasonal variations and mesoscale eddies. The residuals from the final mapped field are almost the same magnitude as the a priori noise indicating that for the upper 3000 dbar the mapped field is statistically consistent with the original data to within the a priori noise (Fig. 2).

Observed salinity and pressure changes on neutral density surfaces

The main water masses along this WOCE section are the shallow salinity maximum (average depth ~245 dbar), the Thermocline Waters between 300 dbar and 700 dbar, the

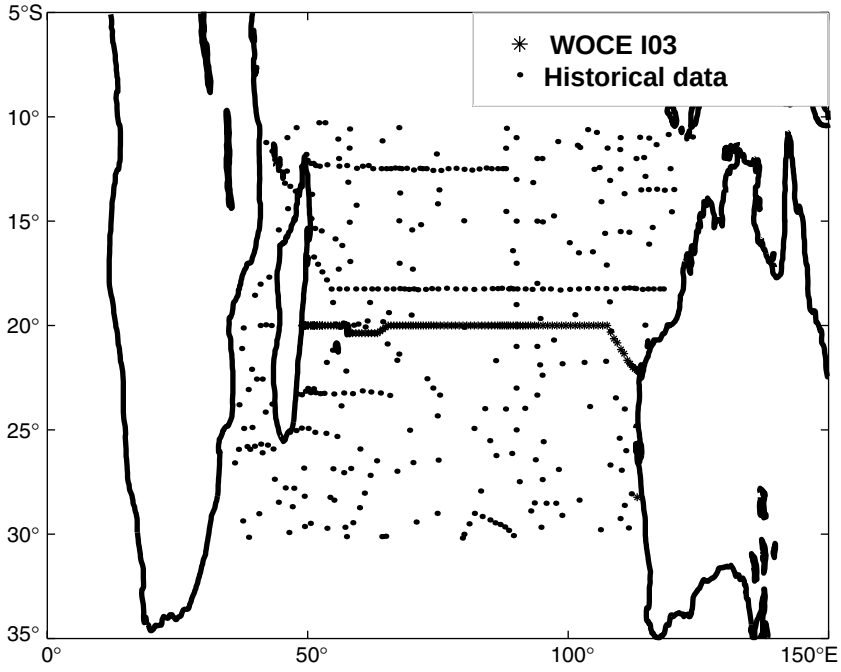

Figure 1. The hydrographic data collected by the RV Knorr for the WOCE I3 section in 1995 (crosses) and the historical data (mean year 1970) used for this analysis (dots).

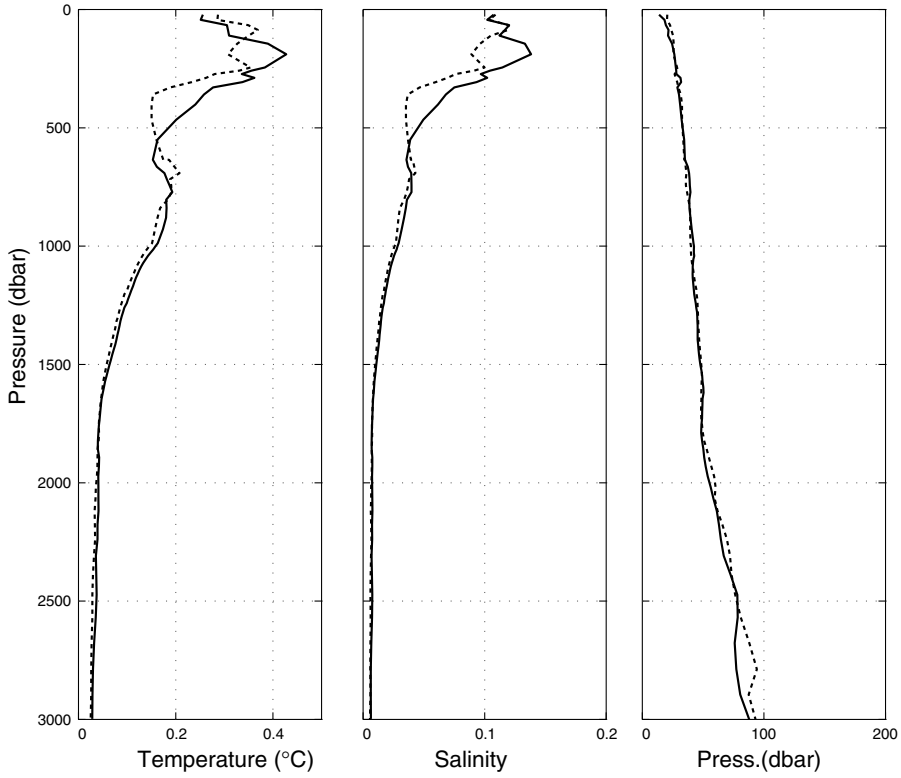

Figure 2. The a priori noise (continuous line) and residual between the interpolated and original historical data (dotted line).

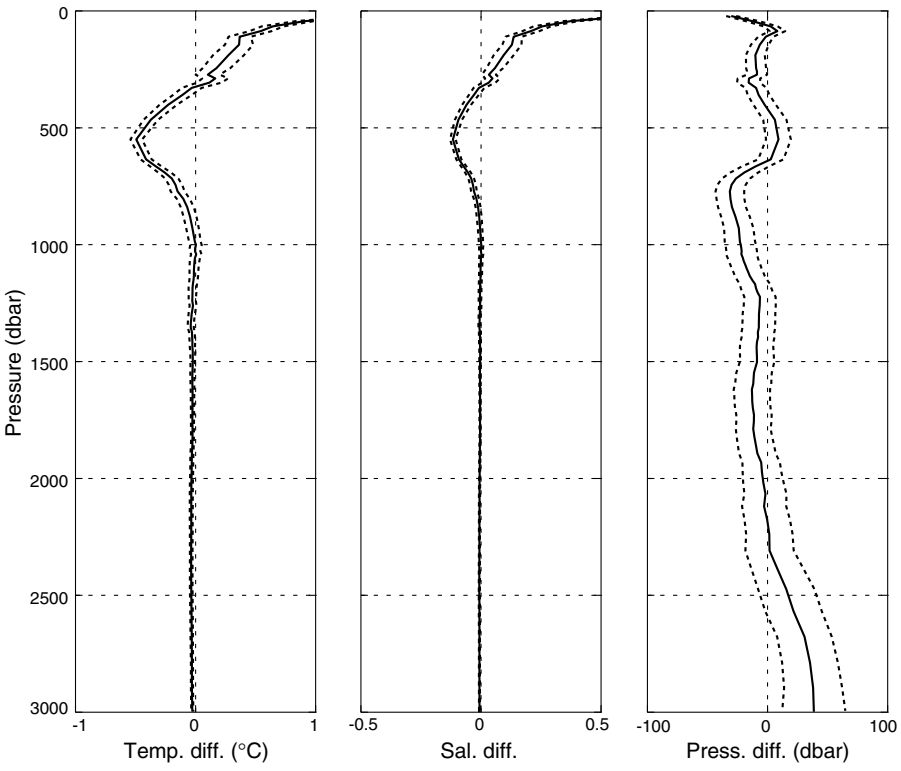

Figure 4. Zonally averaged differences along the section (on neutral density surfaces) between the WOCE I3 section and the interpolated historical data. The pressure coordinate is the zonal average pressure along the WOCE section. The dotted lines are the standard errors estimated for these differences.

Antarctic Intermediate Water (AAIW) characterised by its salinity minimum at an average depth of 800 dbar, and the Circumpolar Deep Water (CDW) characterised by a salinity maximum at an average depth of 2670 dbar.

Fig. 3 (page 16) shows the section differences on neutral surfaces between 1995 and the 1970s along the WOCE I3 section for salinity and pressure. We show only the salinity differences since the temperature differences are correlated through the definition of a neutral surface. This figure shows the salinity on density surfaces has basin wide increases and decreases between Madagascar and Australia within the water column. In the depth range of the shallow salinity maximum (<300 dbar) the salinity (and temperature) has increased on density surfaces. The thermocline waters and upper AAIW have freshened (and cooled) on density surfaces on basin scales (Fig. 3a). Below 1000 dbar the changes in salinity on density surfaces are small and less conspicuous (Fig. 3a).

The differences in depth of density surfaces are not as coherent as the water mass changes along the whole section. The change with the largest length scale occurs in the lower AAIW near 1000 dbar with the density surfaces now shallower. Below 1000 dbar between 55°E and 80°E the density surfaces are shallower, and further to the east between 80°E and 110°E the density surfaces are now deeper (except at 100° to 105°E). This apparent bi-modal variation in the depth of the density surfaces below 1000 dbar suggests a reduction of the zonal slope of the density surfaces and a weakening of the geostrophic circulation.

The large-scale changes are reflected in the zonal averages of the differences. These basin wide differences are the most statis-

tically significant changes compared with the error estimates (Fig. 4). The zonally averaged temperature and salinity have increased above 300 dbar in the shallow salinity maximum water. Below 300 dbar the temperature and salinity have decreased in the thermocline and salinity minimum waters. The freshening at the salinity minimum is 0.02 psu and the maximum difference on density surfaces in the thermocline waters is 0.49°C and 0.12 psu at 550 dbar. The differences in temperature and salinity below 1000 dbar are not significant from our error estimates. Over most of the water column the zonally averaged pressure changes are not statistically significant except below 2500 dbar and between 700 and 1200 dbar. The deep changes suggest that CDW is now deeper but has not significantly changed its water mass characteristics. In the depth range of AAIW density surfaces have shoalled, and at the salinity minimum this depth decrease is 30 dbar. The zonally averaged temperature and salinity diagram shows the overall difference in the water mass properties (Fig. 5). The AAIW is fresher, thermocline waters are fresher and cooler, and the shallow salinity maximum waters are more saline.

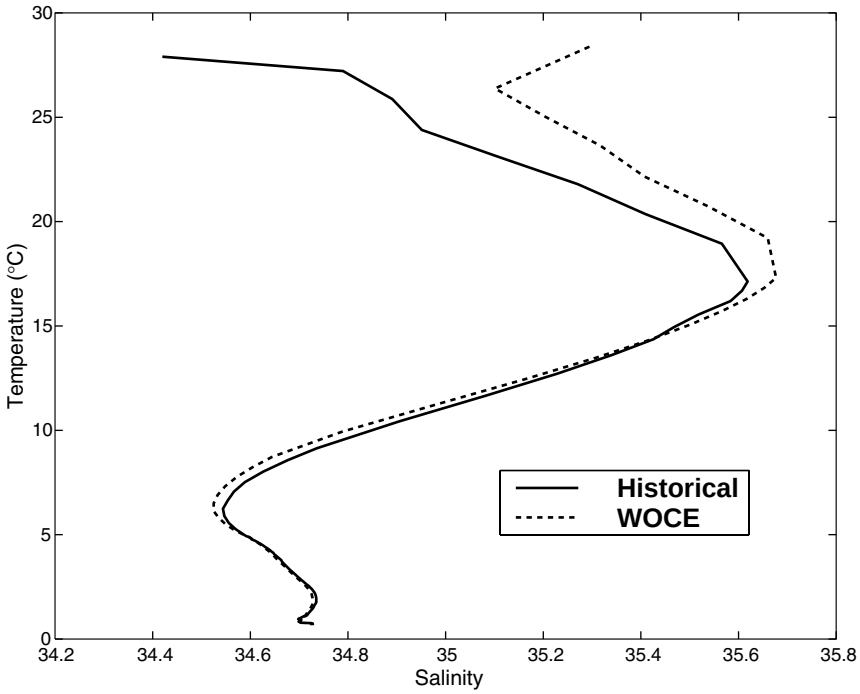

Figure 5. The zonally averaged T-S diagrams (on neutral density surfaces) for the historical data (continuous line) and the 1995 WOCE section (dotted line).

Conclusions

These results are strikingly consistent with the observed changes seen in a similar comparison at 32°S between the WOCE I5 section and the historical data (Bindoff and McDougall, 2000). In that paper the SAMW waters had cooled and freshened on density surfaces. SAMW water occupies the same density range as the thermocline waters of this article. They interpreted the cooling and freshening signal as being most simply explained by the warming of surface waters in the region where SAMW is formed. This interpretation is consistent with the differences reported here for 20°S. Similarly the AAIW had freshened at 32°S but with a greater strength than at 20°S. This weaker freshening signal of AAIW is consistent with the 20°S section being further from the source of AAIW. The shallow salinity maximum layer has become saltier, implying an decrease in precipitation minus evaporation in its source region near 32°S. This result is also similar to that observed in the subtropical Pacific Ocean (Wong et al., 1999). This work is being further extended to the whole Southern Hemisphere to more fully document the changes in global water masses.

References

Bindoff, N. L., and McDougall, T. J., 2000: Decadal changes along an Indian Ocean section at 32°S and their interpretation. J. Phys. Oceanogr., 30, 1207–1222.

Bindoff, N. L., and Wunsch, C., 1992: Comparison of synoptic and climatologically mapped sections in the South Pacific Ocean. J. Climate, 5, 631–645.

Jackett, D., and McDougall, T. J., 1997: A neutral density variable for the world's ocean. J. Phys. Oceanogr., 27, 237–263.

WOCE Data Products Committee, 1998: WOCE Global Data, Version 1.0 CD-ROM; WOCE Rep. 158/98 CD-ROM. WOCE IPO, Southampton, UK.

Wong, A. P. S., Bindoff, N. L., and Church, J. A., 1999: Large-scale freshening of intermediate waters in the Pacific and Indian Oceans. Nature, 400, 440–443.

Wong, A. P. S., Bindoff, N. L., and Church, J. A., 2001: Freshwater and heat changes in the North and South Pacific Oceans between the 1960s and 1985–94. J. Phys. Oceanogr., 31, in press.

Arctic climate variability during 20th century

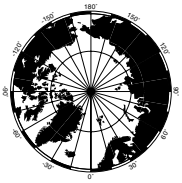

Andrey Proshutinsky, Woods Hole Oceanographic Institution, MA 02543, USA.
aproshutinsky@whoi.edu

Observations and modelling results demonstrate that the recent history of the Arctic is characterised by significant change in the circulation of the Arctic Ocean, (Morrison, 1996; Carmack and Aagaard, 1996); a substantial decrease in sea-ice cover (Maslanik et al., 1996); a significant decrease in the arctic sea level pressure (Walsh et al., 1996); and the changes of the North Atlantic Oscillation (NAO) index (Hurrell, 1995).

To understand the origin of these changes, they need to be placed in the perspective of the record for at least the past hundred years.

Before 1942–1946, most data sets do not cover the central arctic and the Arctic Ocean. Relatively good quality observations at high latitudes exist in quantity only after 1978 when satellite measurements and surface ice buoys (International Arctic Buoy Program) began coverage of the polar regions. Therefore, one of the goals of this paper is data reconstruction for the Arctic region using different approaches, assumptions and physical relationships. This paper also overviews variability of atmospheric and oceanic parameters during the 20th century based on existing observations and model results.

Sea surface atmospheric pressure (SLP)

Monthly mean gridded ($5° \times 5°$) SLP data (NCAR data support section, "Trenberth data set") covers the period from 1899 through 1999. There are no data for latitudes 75°N, 85°N and North Pole for 1899–1942. To reconstruct this information we have used two methods. The first one is based on EOF analysis and the second method, which we call "analogy method", is briefly described below.

An SLP field with missing data (before 1943) was compared with each SLP field after 1943, and a sum of square differences between these fields (for the all latitudes with existing data) was calculated for reconstruction purposes. The SLP with the minimum sum we recognise as a SLP-analogue for the field we want to reconstruct. This procedure allows us to generate a table where each SLP before 1943 has its analogue among SLPs after 1943. Finally for 100-year analysis, the SLP field with missing data has been substituted with the SLP-analogue field.

This procedure allows us to establish the first order similarity between atmospheric processes before and after 1943. Fig. 1a (page 16) shows the 5-year running mean observed (solid line) and reconstructed (dashed line) SLPs for the North Pole and Iceland. One can see that the reconstructed data practically coincides with the observed data in Iceland. This fact allows us to conclude that the reconstructed SLP at the North Pole is reasonable. Fig. 1a shows that the SLP at the North Pole and over the Arctic Ocean (not shown) is decreasing from the beginning of the century with the maximum decrease at the North Pole (1 mb per decade). The decadal scale variability in the SLP is well pronounced in addition.

Surface air temperature (SAT)

This data set is a combination of land air temperature anomalies (Jones, 1994) and sea surface temperature anomalies (Parker et al., 1995) on a $5° \times 5°$ grid-box basis. The merging of the two data sets is discussed in Parker et al. (1995). Both components of the data set are expressed as anomalies from 1961–1990. The data set has been extensively used in the various Intergovernmental Panel on Climate Change (IPCC) reports. Fig. 1c shows annual mean air temperature anomalies averaged for latitudes 65°N–90°N (blue and read bars) and 5-year running mean variability (black solid line). There were two cold and two warm climate states during 20th century and there is a trend of about 0.8°C per 100 years. One can see that significant arctic warming was observed in the 1920s–1940s and that the SAT anomalies were higher than we have observed recently. It is also important to take into account that the density of observations during the first part of the century was significantly lower, and these observations represent mainly the western part of the Arctic (including the Norwegian, Greenland, and Barents Seas and surrounding land stations).

Sea ice conditions

Monthly mean $1° \times 1°$ sea ice concentration from 1899 through 1998 is available from Active Archive Data Center, National Center for Atmospheric Research (NCAR). This data-set is a compilation of data from several sources integrated into a single gridded product by John Walsh and Bill Chapman, University of Illinois. These sources of data have changed over the years from observationally derived charts to satellite data. Gaps within observed data are filled with climatology or other numerically derived data.

Fig. 1b shows sea ice area (SIA) variability from this source (solid black line depicts 5-year running mean data). One can see a dramatic decrease in SIA since approximately 1950. A comparison among Figs. 1a, 1b and 1c shows that after 1950 the SIA correlates very well with SAT (Fig. 1b), i.e. cold 1960s–1970s correspond to increase in SIA, and warm 1980–1990s are in good correlation with significant decrease in SIA. Before 1950s, there is no correlation between SAT and SIA. This is probably because of many gaps and uncertainties in sea ice conditions for that time. We have reconstructed sea ice conditions based on results of our SLP reconstruction assuming that each monthly SLP field has its own ice distribution pattern. This is possible

because sea-ice conditions correlate very well with wind conditions. This assumption allows us to use Table 1 for reconstruction of SIA. We substitute monthly SIAs before 1946 by their analogues after 1946. The results of this reconstruction is shown by red dotted line in Fig. 1b. One can sea that now, the SIA has much more decadal variability during 1899–1945 then in the Walsh's data, and that this variability is consistent with SAT variability. There is maximum in SIA at the beginning of the century when SAT anomalies were negative. During 1920s–1940s, when the arctic SAT anomalies were high, the SIA was significantly less than normal. Based on reconstructed data we conclude that SIA has been reducing during 20th century with a rate of about 1E6 square km per 100 years with very well pronounced interannual and decadal variability after 1940s.

Precipitation

A historical monthly precipitation data set for global land areas from 1900 to 1998, gridded at $2.5° \times 2.5°$ resolution has been constructed by M. Hulme (1992) and is available for scientific purposes. Fig. 1d shows variability of precipitation anomalies averaged over area 65°N–90°N. This figure reflects only land areas and does not include any information about precipitation regime over oceans. One can conclude that precipitation has been increasing during 20th century with a linear trend of 30 mm per 100 years in the Arctic.

River discharge

Approximately 50-year time series (typically 1936–1990) of river discharge at stations along Eurasian and Alaskan Arctic coasts are available from the Environmental Working Group Atlas of the Arctic Ocean (EWG, 1998). River discharge figure (1e) is consistent with precipitation regime (Fig. 1d) but positive trend is not so well pronounced as in precipitation anomalies.

Sea level

About 60 tide-gauge stations in the Kara, Laptev, East-Siberian and Chukchi Seas have recorded the sea level change from the 1950s through 1990s. Over this 40-year period, most of these stations show a significant sea level rise (see Fig. 1f). The sea level data were collected by the Arctic and Antarctic Research Institute, St. Petersburg, Russia. Some information about this data set can be found in the Environmental Working Group (EWG) Atlas of the Arctic Ocean (1998). Blue lines in Fig. 1f show annual mean sea level from observations (thin line) and linear trend (thick line). Dotted red line depicts annual mean sea level from numerical simulation based on reconstructed SLP discussed above. Model description, calibration and design of numerical experiments were discussed by Proshutinsky and Johnson (1997). The observed and simulated sea surface heights are in good agreement, and simulated positive trend in sea level corresponds to the observational trend very well. The sea level rises in the Arctic Ocean with a trend of about 10 cm per 100 years. Our studies (Proshutinsky, 2000; Proshutinsky et al., 2000) have shown that observed sea level increase can be explained by changes in thermohaline and wind-driven circulation of the Arctic Ocean and by decreasing of atmospheric pressure in the Arctic.

Ice and ocean circulation

Proshutinsky and Johnson (1997), Proshutinsky et al. (1999) simulated the vertically averaged currents, sea level heights, and ice drift in the Arctic Ocean from 1946 to 1999 using a two-dimensional, wind-forced, barotropic model that includes frictional coupling between the ocean and ice. The model has a spatial resolution of 55.5 km and is driven by winds calculated from NCAR SLPs, river run-off, and an imposed but realistic sea level slope between the Pacific and the Atlantic Oceans. There is a good agreement between velocities from observed buoy motions and velocities of modelled ice drift even though the model lacks ocean baroclinicity and ice thermodynamics. The results indicate that the wind-driven motion in the central Arctic alternates between anti-cyclonic and cyclonic circulation with each regime persisting for five to seven years, based upon our analysis of the modelled sea level and ice motion. Anti-cyclonic wind-driven motion in the central Arctic appeared during 1946–1952, 1958–1963, 1972–1979, and 1984–1988, 1998–present, and cyclonic motion appeared during 1953–1957, 1964–1971, 1980–1983, and 1989–1997. Shifts from one regime to another are forced by changes in the location and intensity of the Icelandic low and the Siberian high. These transformations from one regime to another can be defined as climate shifts in the Arctic Ocean and occur quite rapidly. Fig. 2 (upper panel) shows typical distribution of SLP, ice and surface currents in the Arctic Ocean for the anticyclonic (left) and cyclonic (right) circulation regimes. Based on reconstructed monthly mean SLPs we have simulated ice drift and ocean circulation for 1899–1999.

A time series of simulated sea level gradients (Fig. 2, lower panel, bars) was constructed according to the procedure described in Proshutinsky and Johnson (1997) (see section 3.2, page 12505 and Figs. 8–10). Positive sea level gradients (Fig. 2) mean that the sea level in the centre of the Arctic Basin is higher than along coastline and that the circulation is anticyclonic (clockwise). Negative sea level gradients have a lowered central sea level and increased

Table 1. SLP analogues, examples of

Original SLP	SLP analogue
January 1899	January 1961
February 1899	February 1983
March 1899	March 1951
and so on…	
December 1942	December 1997

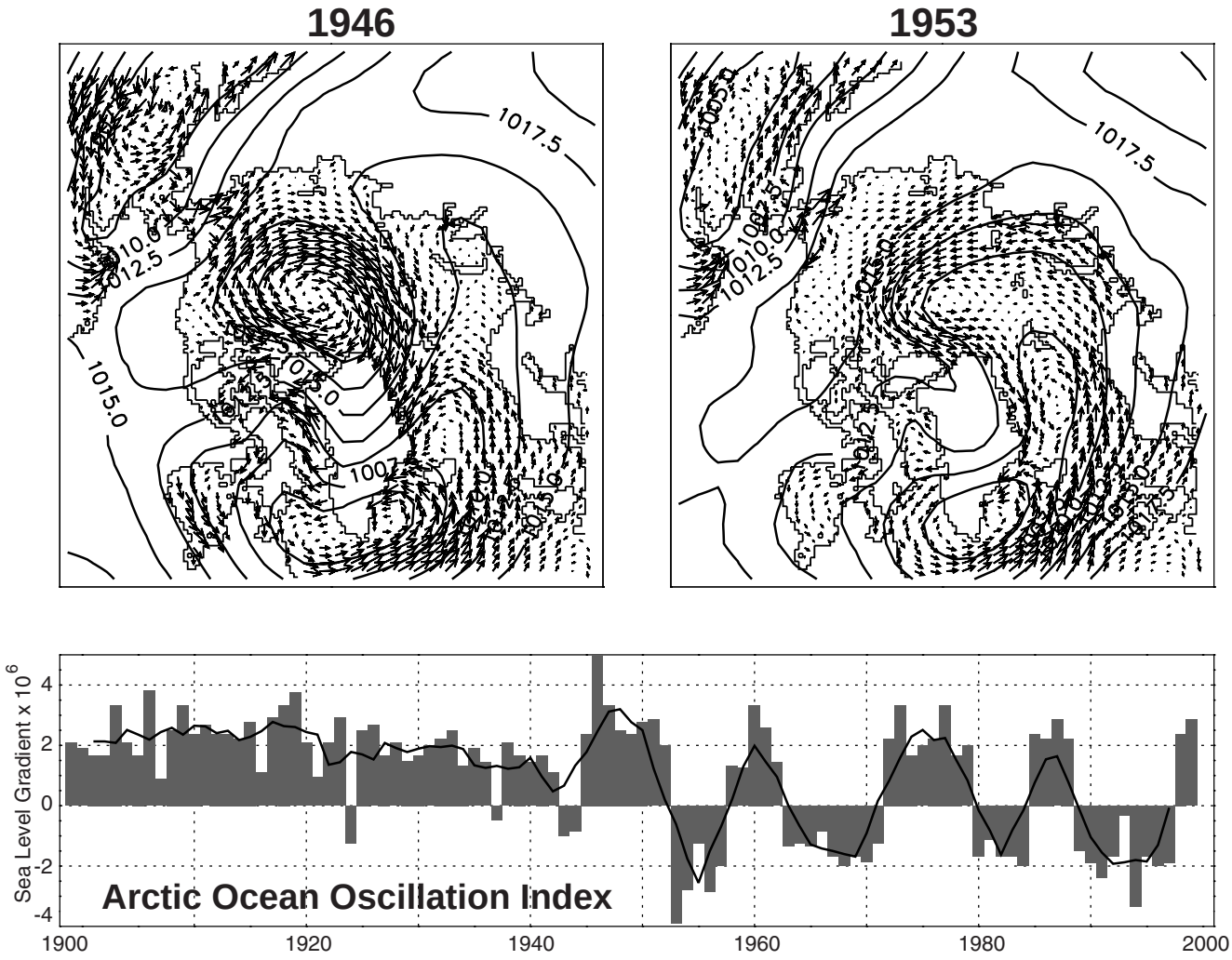

Figure 2. Upper panel shows distributions of SLP (mb) and ice and ocean surface circulation for the anticyclonic (left) and cyclonic (right) circulation regimes. The lower panel is a time series of sea level gradients (vertical bars) in the central Arctic Basin with positive values indicating anti-cyclonic circulation and negative values indicating cyclonic circulation. This time series serves as Arctic Ocean Oscillation index for our analysis.

sea level along coastline, and the circulation is cyclonic (counterclockwise). From Fig. 2 we conclude that before 1942, the strong anticyclonic circulation regime dominated over the Arctic Ocean and after 1942 we have observed four anticyclonic and four cyclonic regimes as described above. Detailed analysis of observational data and results of numerical experiments revealed significant differences in atmospheric, ice, and oceanic parameters during these two climate states. During the anticyclonic circulation regime, "winter" conditions with a cold and dry atmosphere, increased ice thickness and ice concentration, and a saltier and colder upper ocean, prevail in the seasonal cycle. During the cyclonic circulation regime, "summer" conditions dominate with a relatively warm and wet atmosphere, reduced ice thickness and ice concentration and ice extent, and a fresher and warmer ocean (Proshutinsky et al., 1999; Polyakov et al., 1999). Based on our most recent results we confirm (as it was predicted 2 years ago) that the cyclonic climatic regime (1989–1997) changed to an anticyclonic regime in 1998 and we expect some cooling in the Arctic with increased ice thickness, ice concentration and ice extent during next 5–7 years.

References

Carmack, E. C., and K. Aagaard, 1996: The dynamic Arctic Ocean: Spatial, temporal, and conceptual heterogeneities. Abstract. Eos, Transactions, AGU, 76, 3, OS12.

EWG (Environmental Working Group), 1997, 1998. Joint U.S.-Russian Atlas of the Arctic Ocean (CD-ROM). National Snow and Ice Data Center, Boulder, Colorado.

Jones, P. D., 1994: Hemispheric surface air temperature variability – A reanalysis and update to 1993. J. Climate, 7, 1794–1802.

Hulme, M., 1992: A 1951–80 global land precipitation climatology for the evaluation of general circulation models. Climate Dyn., 7, 57–72.

Hurrell, J. W., 1995: Decadal Trends in the North Atlantic Oscillation: Regional Temperatures and Precipitation. Science, Vol. 269, 676–679.

Maslanik, J. A., M. C. Serreze, and R. G. Barry, 1996: Recent decrease in summer Arctic ice cover and linkages to anomalies in atmospheric circulation. Geophys. Res. Lett. 23(13), 1677–1680.

Morrison, J. E., 1996: Changes in upper ocean hydrography measured during the 1993 cruise of the USS Pargo. Abstract. Eos, Trans., AGU, 76(3), OS12.

Parker, D. E., C. K. Folland, and M. Jackson, 1995: Marine surface temperature: observed variations and data requirements. Clim. Change, 31, 559–600

Polyakov, I. V., A. Y. Proshutinsky, and M. Johnson, 1999: Seasonal cycles in two regimes of Arctic climate. J. Geophys. Res., 104, C11, 25761–25788.

Proshutinsky, A. Y., and M. A. Johnson, 1997: Two circulation regimes of the wind-driven Arctic Ocean. J. Geophys. Res., 102, 12493–12514.

Proshutinsky, A., I. Polyakov, and M. Johnson, 1999: Climate states and variability of Arctic ice and water dynamics during 1946–1997. Polar Research, 18(2), 135–142.

Proshutinsky, A., 2000: Arctic climate oscillation from observations and model results, EGS Meeting, Nice, France, April 25–27, 2000.

Proshutinsky, A., V. Pavlov, and R. Bourke, 2000: Sea level rise in the Arctic Ocean, GRL, submitted.

Walsh, J. E., W. L. Chapman, and T. L. Shy, 1996: Recent decrease of sea level pressure in the central Arctic. J. Climate, 9, 480–486.

Subsurface subtropical fronts of the North Pacific as boundaries in the ventilated thermocline

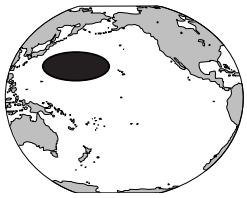

Yoshikazu Aoki, Toshio Suga, and Kimio Hanawa, Tohoku University, Japan.
aoki@pol.geophys.tohoku.ac.jp

An eastward upper flow in the central subtropical gyre of the North Pacific and an accompanying subsurface temperature/density front have been documented by many authors (e.g., Uda and Hasunuma, 1969), which were often referred to as Subtropical Countercurrent and Subtropical Front. While early studies suggested that this countercurrent/front could be caused by a local wind structure (e.g., Yoshida and Kidokoro, 1967; Cushman-Roisin, 1981), Takeuchi (1984) concluded that the local wind distribution is not essential based on his numerical experiment using an

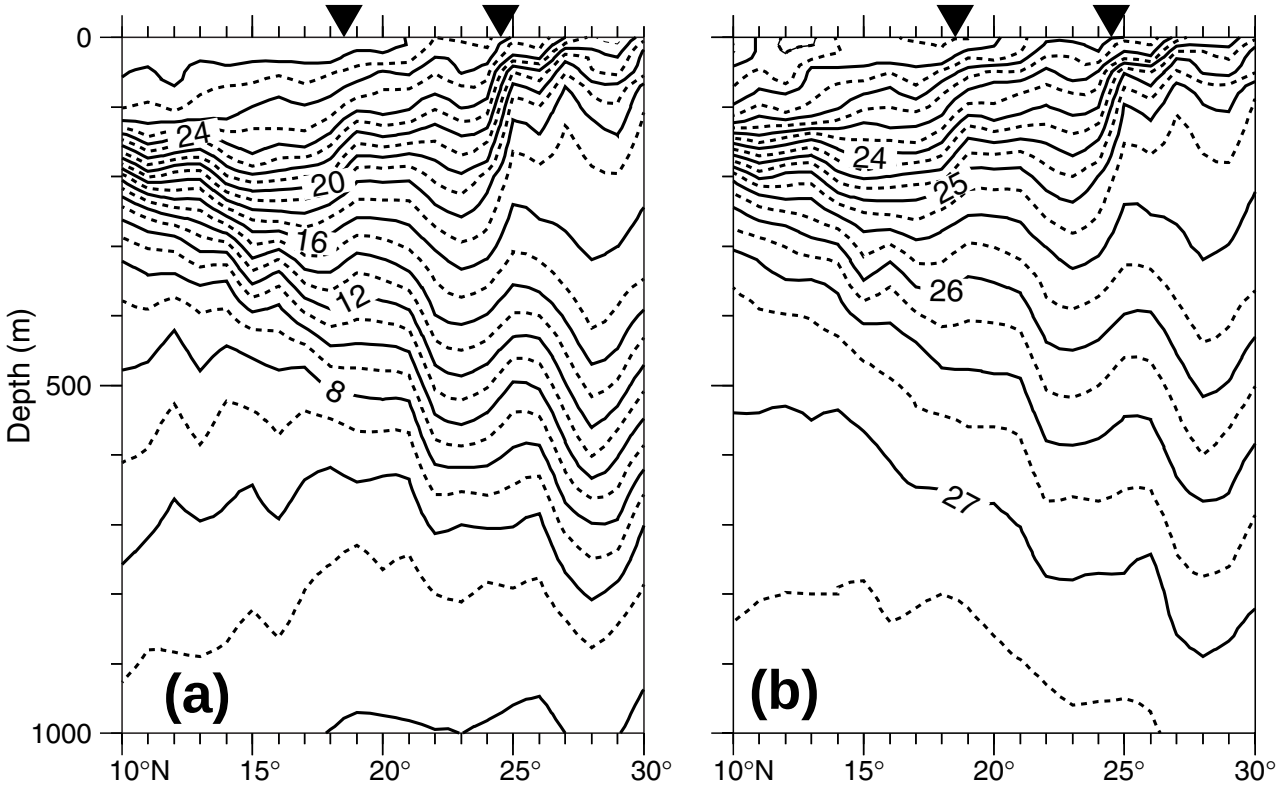

Figure 1. (a) Potential temperature and (b) potential density sections observed in June 1977 along 155°E repeat line. Inverted triangle marks the frontal position.

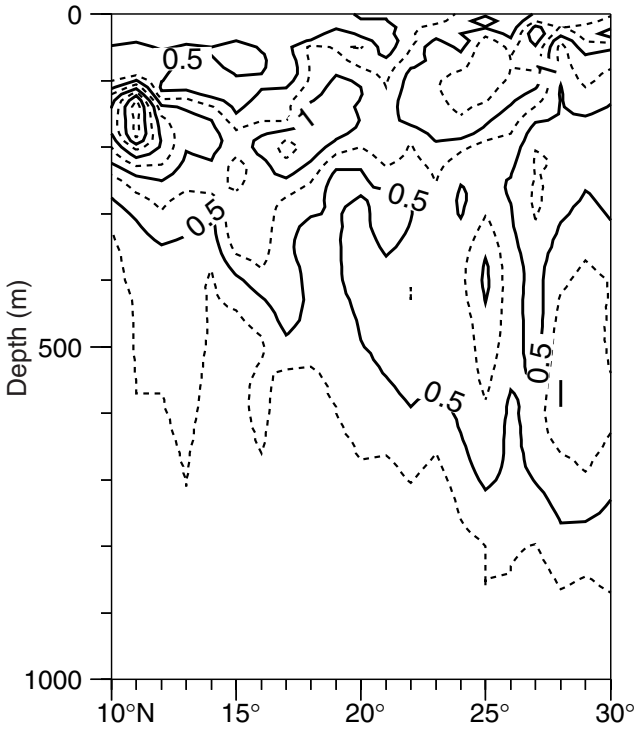

Figure 2. Latitude-depth distribution of the standard deviation of potential temperature over 9 observations along 155°E repeat line.

ocean general circulation model.

Recently, Kubokawa and Inui (1999) and Kubokawa (1999) suggested that low potential vorticity water subducted and advected from the northern part of the gyre can cause the countercurrent/front. In the light of these new studies, the countercurrent/front can be inherently related to the structure of the ventilated thermocline. The present study attempts to document detailed hydrographic structure of the subsurface countercurrent/front and clarify its significance in the ventilated thermocline.

Analysis and results

Long-term repeat hydrographic sections along 130°E, 137°E, 144°E and 155°E capture two subsurface temperature/density fronts and associated eastward currents near 24°N and 18°N on the average. For example, the two fronts are indicated at 24.5°N and 18.5°N along 155°E in June 1977 (Fig. 1). The section of the temperature standard deviation from 9 cruises along 155°E also exhibits two maxima associated with the frontal variability at 24°N and 100 m, and 18°N and 200 m (Fig. 2). The northern front corresponds to Subtropical Front mentioned above; the southern front also has been noticed in literature (Nitani, 1972; Hasunuma and Yoshida, 1978) but hardly followed up so far.

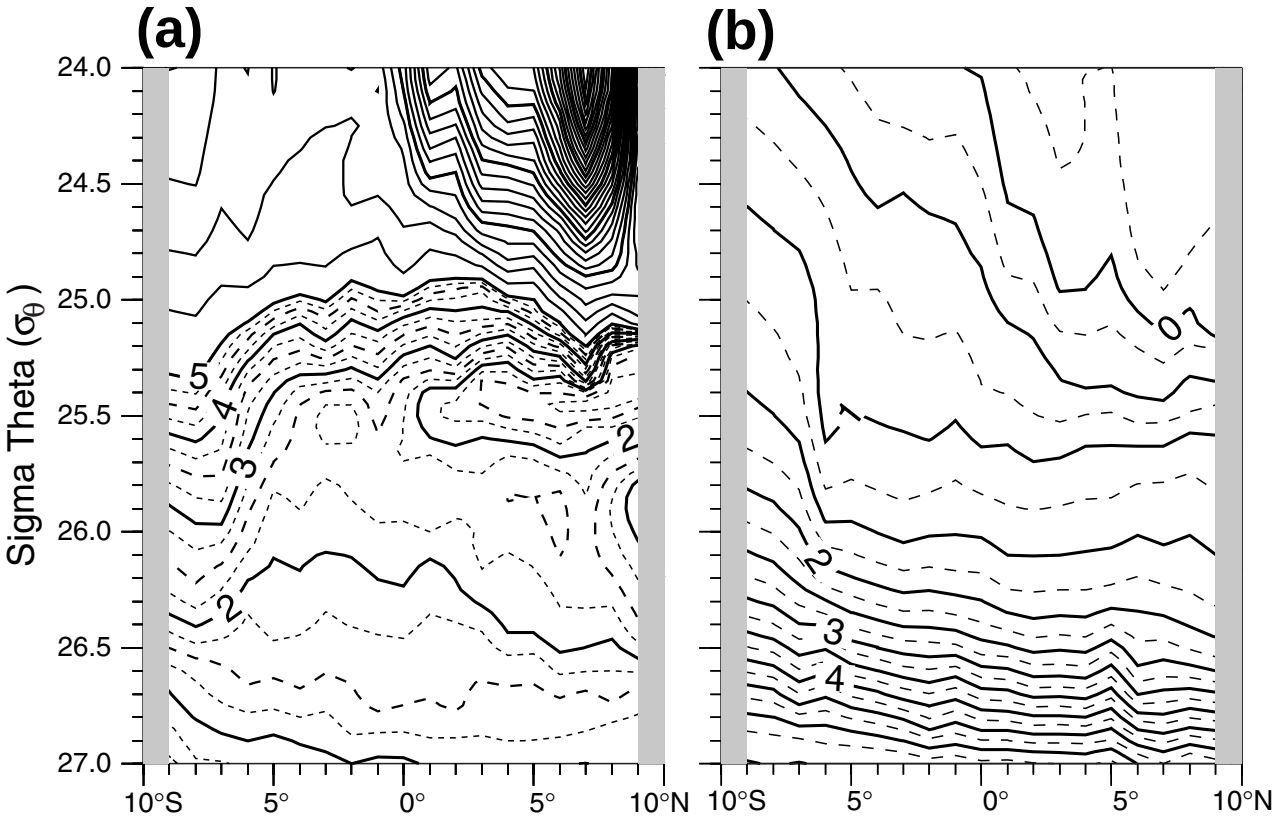

Figure 3. Mean sections based on the frontal coordinates of (a) PV and (b) AOU with respect to the northern front along 155°E repeat line.

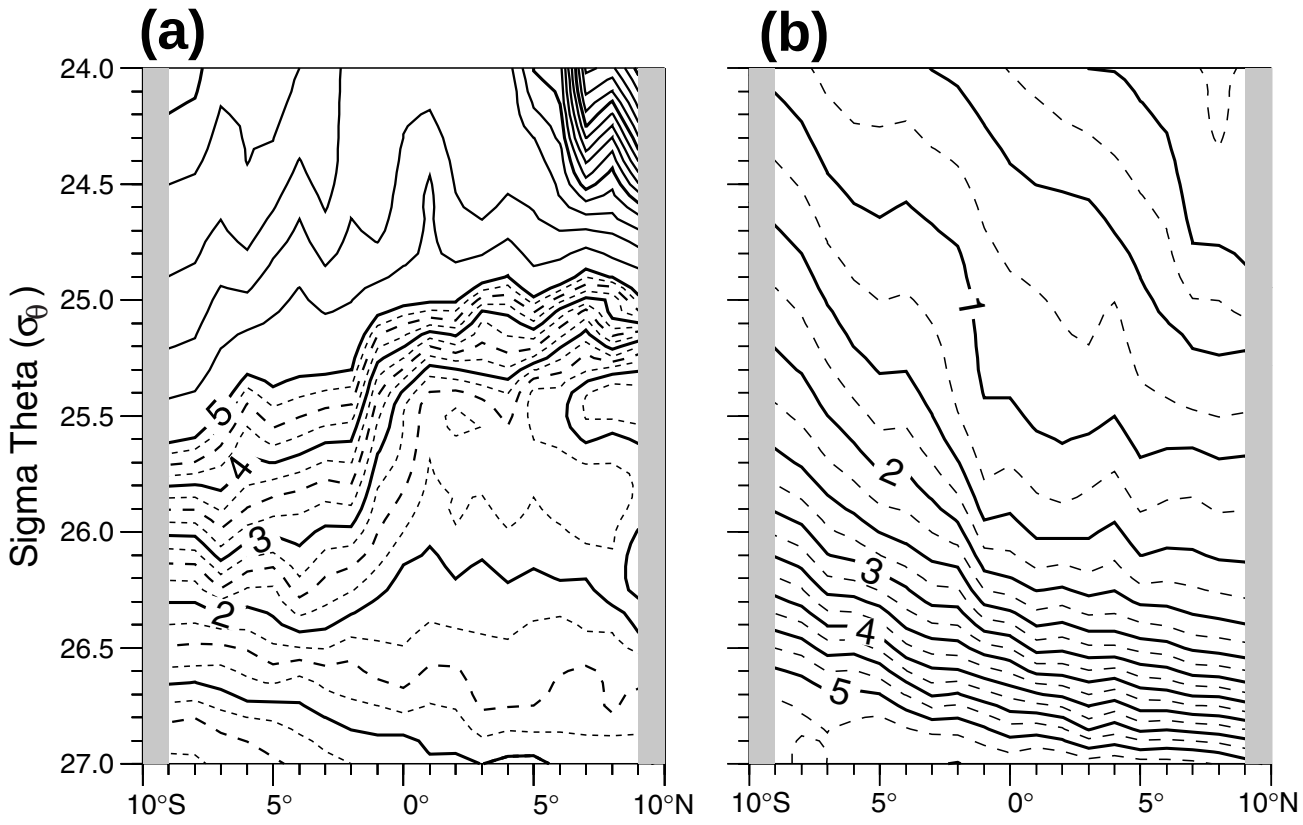

Figure 4. Mean sections based on the frontal coordinates of (a) PV and (b) AOU with respect to the southern front along 155°E repeat line.

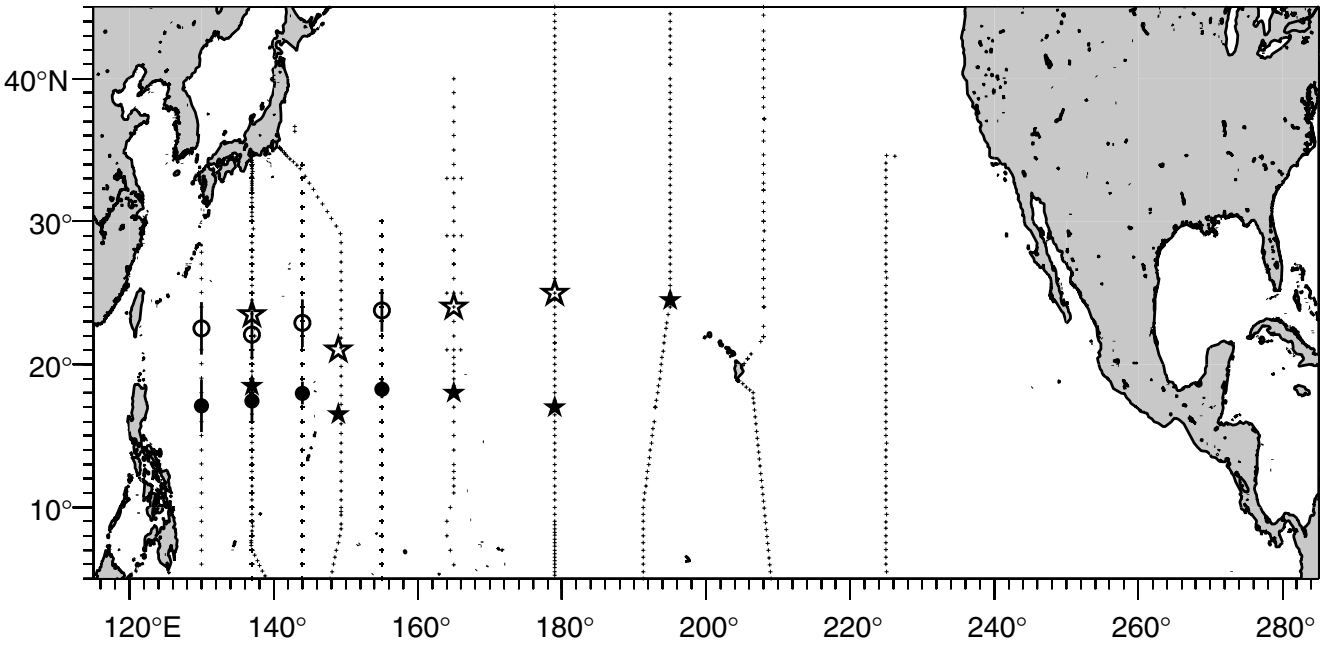

Figure 5. Positions of the subsurface subtropical fronts along the repeat lines and the WOCE/WHP lines. The mean positions and the associated standard deviations are indicated by circles and straight lines, respectively. The frontal positions along the WOCE/WHP lines are indicated by stars. The northern and southern fronts are shown in open and closed symbols, respectively. Observational stations are marked by small dots.

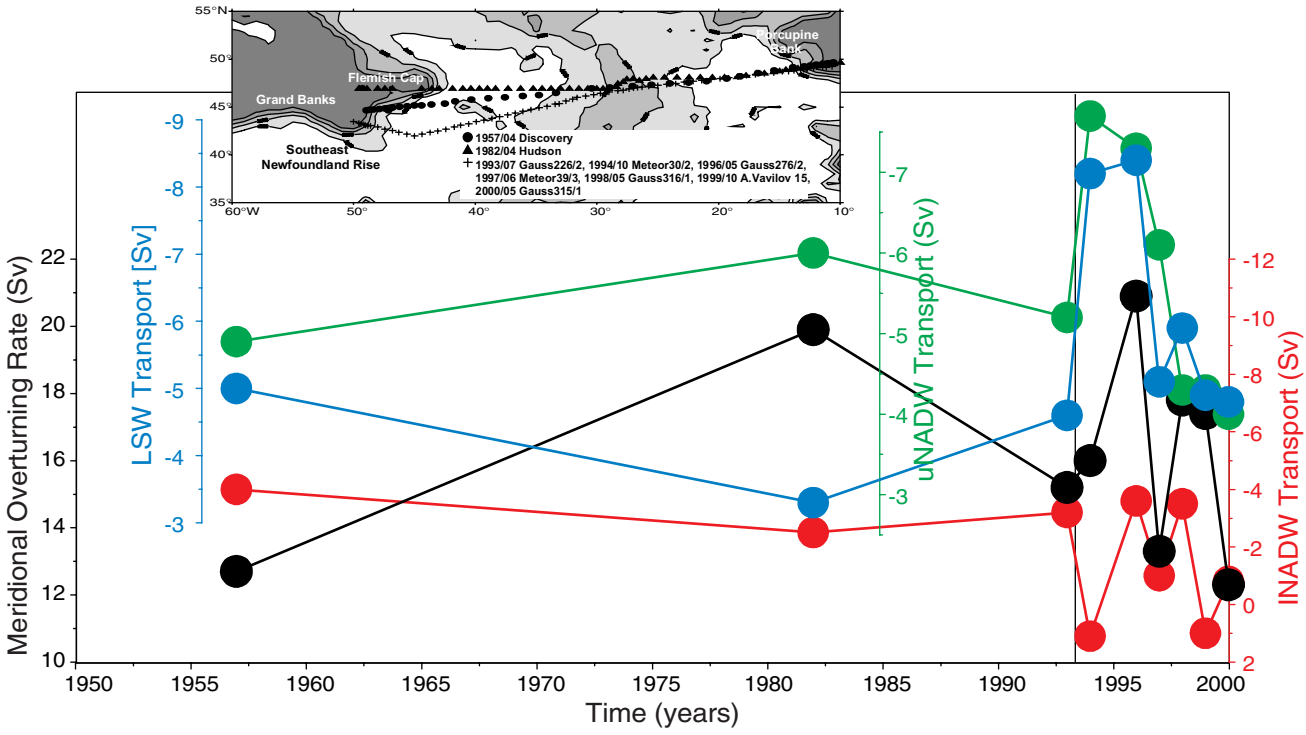

Lorbacher and Koltermann, page 3, *Figure 1. Hydrographic sections between 42°–49°N in the North Atlantic during the Period 1957–2000 and volume transports of water masses across these sections defined for distinct different intervals of neutral density* γ^n. *The transports are positive northward and negative southward, respectively.*

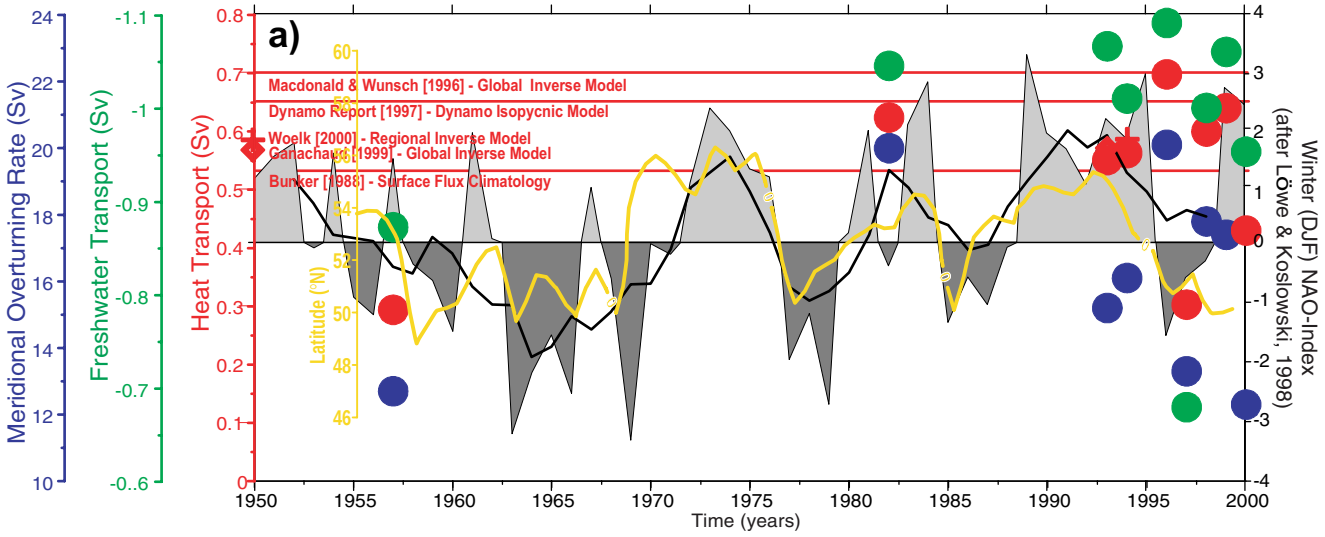

Lorbacher and Koltermann, page 3, *Figure 2. "Time series" of the winter (DJF) NAO-index after Löwe and Koslowski (1998) and of the meridional overturning rate across "48°N" in the North Atlantic and the total meridional heat and freshwater transports, respectively. Black line: five year running mean of the NAO-index. Yellow line: line of zero* $curl_z\vec{\tau}$ *(zonally-integrated between 10°–30°W in Winter (DJF)).*

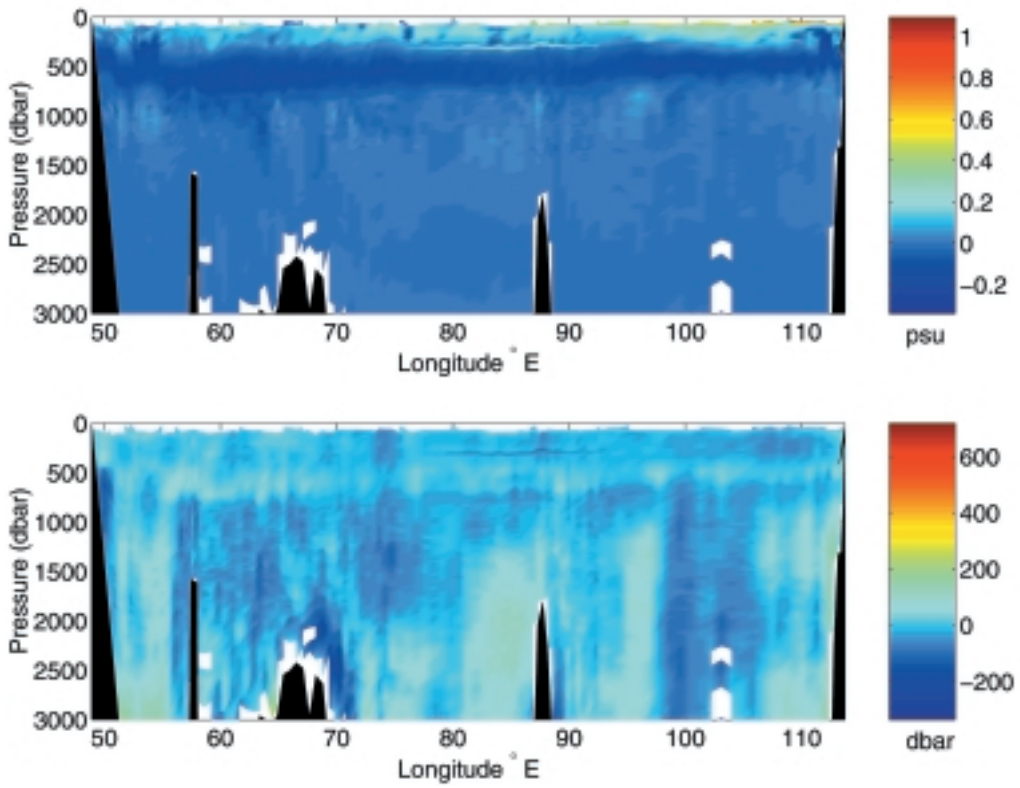

Howe, page 6, *Figure 3. (a) Salinity differences (on neutral surfaces) between the WOCE section and the interpolated historical data. The depth ordinate is the zonal average pressure along the WOCE section of each neutral density surface used in the analysis. Positive differences indicate an increase in salinity on the density surfaces (upper panel). (b) Pressure differences (on neutral surfaces) between the WOCE section and the interpolated historical data. The depth ordinate is the zonal average pressure along the WOCE section of each neutral density surface used in the analysis. Positive differences indicate an increase in pressure on the density surfaces (that is deeper) (lower panel).*

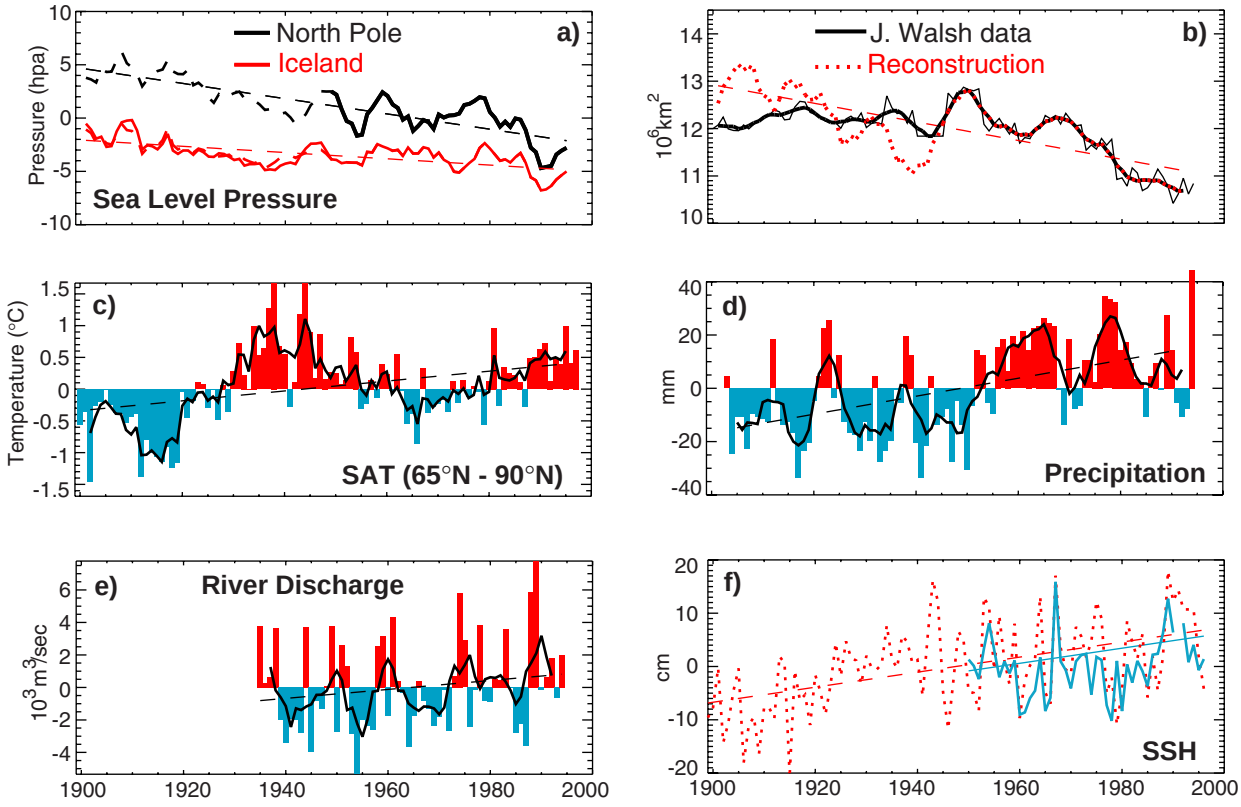

Proshutinsky, page 9, *Figure 1. Observed (solid lines and bars) and reconstructed (dotted lines) environmental parameters for the Arctic region.*

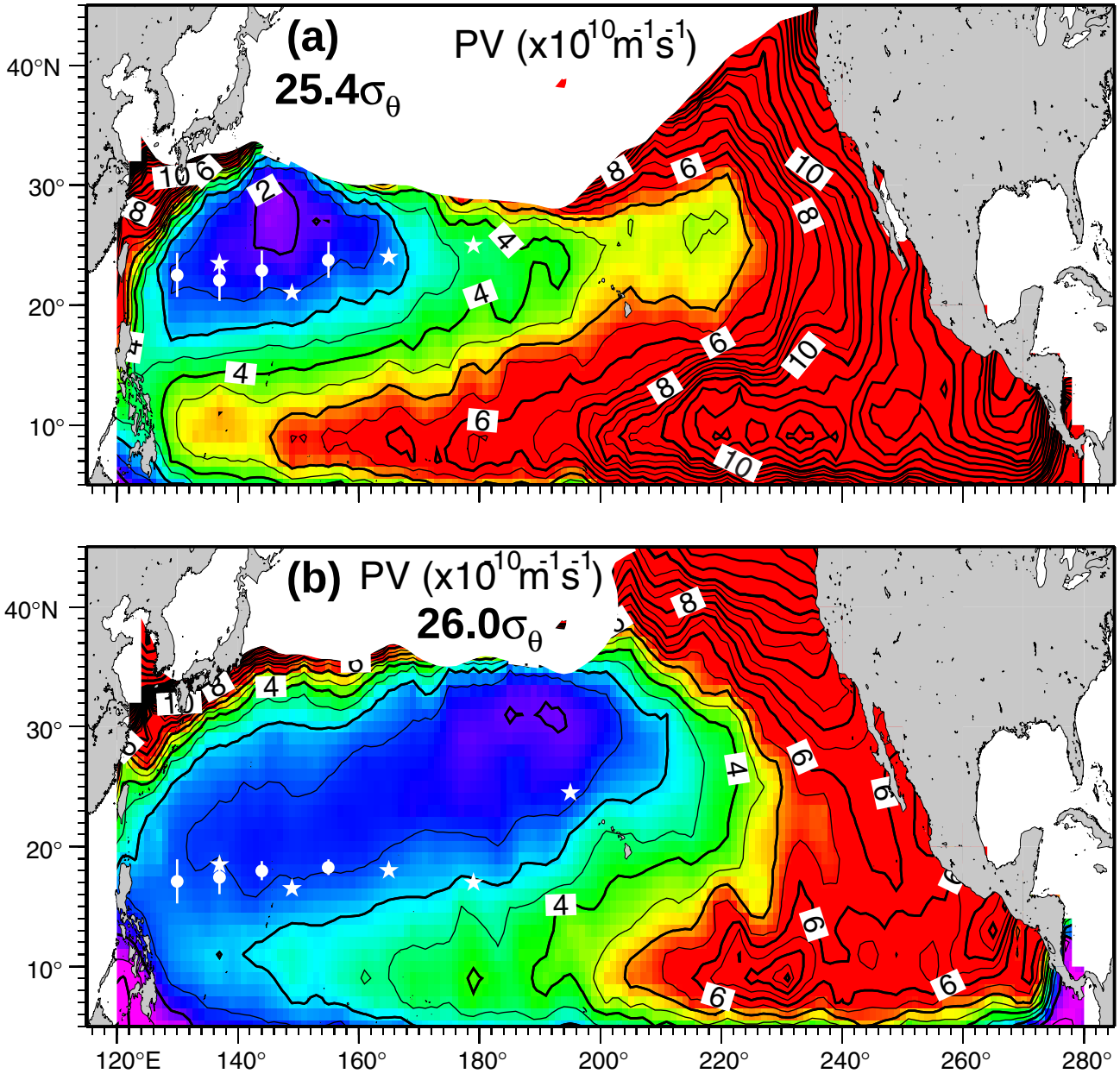

Aoki et al., page 12, *Figure 6. PV maps on (a) 25.4 σ_θ and (b) 26.0 σ_θ isopycnal surface. These maps are drawn by using an isopycnally averaged climatology: North Pacific HydroBase (Macdonald et al., 2000). A winter outcropping region is excluded. The positions of the northern front and the southern front shown in Figure 4 are surperposed in (a) and (b), respectively.*

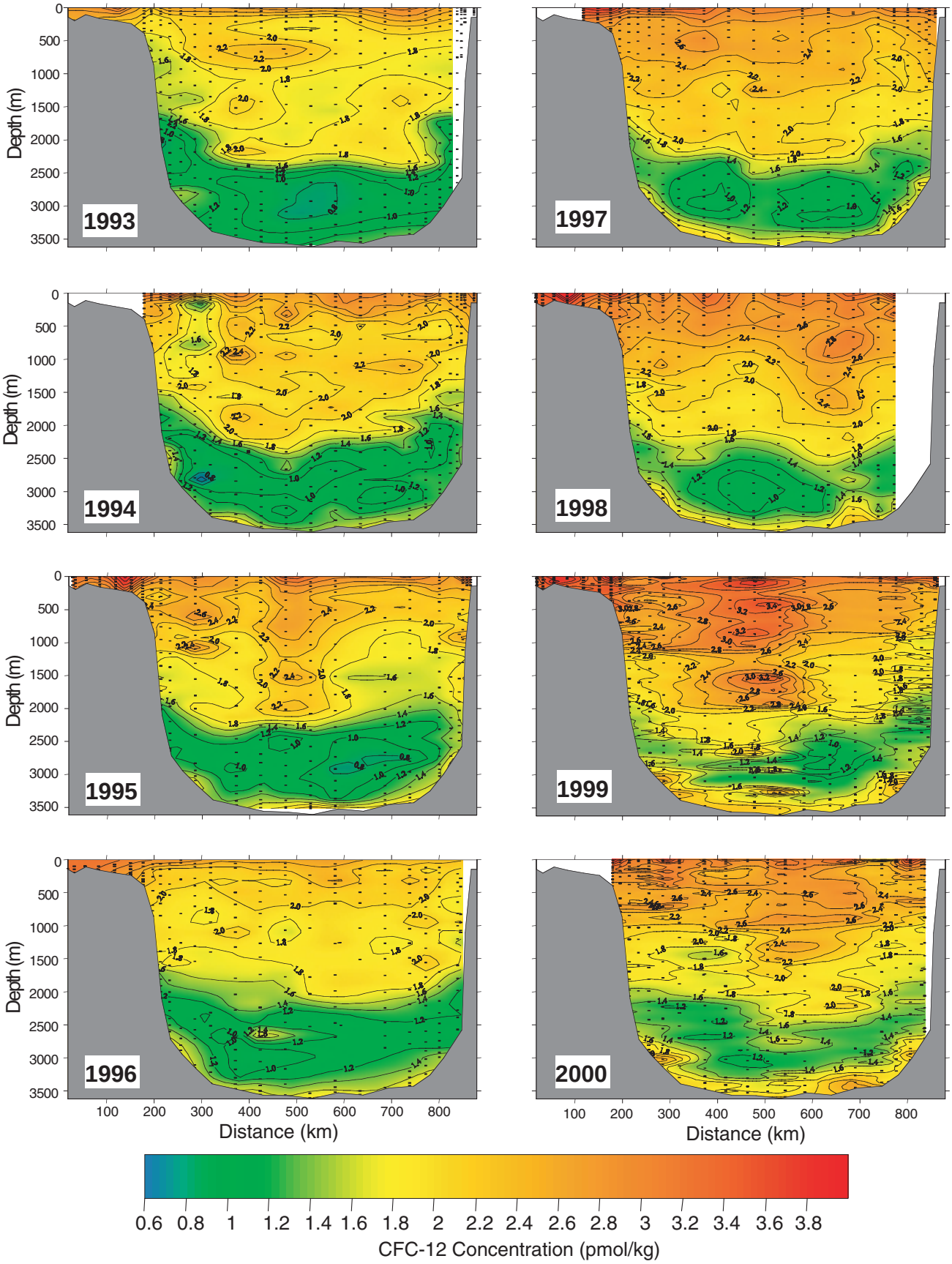

Azetsu-Scott et al., page20, *Figure 2. CFC-12 distribution along the WOCE AR7W line from 1993 to 2000. Three water masses at the central Labrador Sea are identified with the CFC-12 concentration in LSW>DSOW>NEADW. General increase of CFC-12 concentration in the Labrador Sea is observed with time.*

In order to extract typical hydrographic features across each of the two fronts, mean fields for each repeat section are calculated using frontal coordinates. The northern (southern) frontal position is detected in all individual sections as a location of maximum meridional gradient of vertically averaged temperature over 100–200 m layer in the latitudinal range of 20–26°N (14–20°N). The mean sections with respect to the northern front (e.g., Fig. 3) show that the water of low potential vorticity (PV) less than $2\times10^{-10}\ \mathrm{m^{-1}\,s^{-1}}$ centred at 25.4 σ_θ extends southward from the northern end of the section to the poleward flank of the front. Apparent oxygen utilisation (AOU) is also lower to the north of the front. This low PV/AOU water corresponds to new North Pacific Subtropical Mode Water (NPSTMW) (e.g., Suga and Hanawa, 1995). On the other hand, the mean sections regarding the southern front (e.g., Fig. 4) demonstrate that the front bounds southward extent of the lower PV/AOU water to the north in the wide density range of 25.3–26.2 σ_θ. The major portion of this low PV/OU water corresponds to North Pacific Central Mode Water (NPCMW) (e.g., Suga et al., 1997).

The positions of the subsurface fronts coinciding with the PV/AOU boundaries described above are sought in the WOCE/WHP meridional sections along 137°E, 149°E, 165°E, 179°E, 165°W, 153°W and 135°W. All the frontal positions detected along the WOCE/WHP and the repeat sections show in Fig. 5. It appears that the both northern and southern fronts are zonally consecutive features. The northern front near 24°N extends eastward as far as the date line. The southern front extends to 165°W with shifting northward to the east of the date line.

The spatial distributions of the fronts are consistent with the southward extent of the relevant low PV water as shown in Fig. 6 (page 17). On the 25.4 σ_θ surface, the low PV of NPSTMW dominates the recirculation region in the western basin, and the northern front is located close to the southern boundary of the low PV core. On the 26.0 σ_θ surface, the low PV associated with NPCMW appears to extend along the subtropical interior flow. The southern front corresponds with the southern limit of the low PV associated with NPCMW.

Conclusions and remarks

The two subsurface basin-wide temperature/density fronts in the subtropical North Pacific are confirmed. The northern front around 24°N and the southern one around 18°N correspond with the southern limits of the low PV associated with NPSTMW and NPCMW, respectively. These features are consistent with the formation mechanism of Subtropical Front proposed recently (Kubokawa, 1999). Although further study is needed to clarify the mechanism of the frontogenesis, it is apparent that the fronts correspond to the boundaries between the distinct regions with different ventilation history. It will thus be useful to monitor these fronts for better understanding of the upper oceanic ventilation and its variability.

References

Cushman-Roisin, B., 1981: Effects of horizontal advection on upper ocean mixing: A case of frontogenesis. J. Phys. Oceanogr., 11, 1345–1356.

Hasunuma, K., and K. Yoshida, 1978: Splitting of the subtropical gyre in the western North Pacific. J. Oceanogr. Soc. Japan, 34, 160–172.

Kubokawa, A., 1999: Ventilated thermocline strongly affected by a deep mixed layer: A theory for subtropical countercurrent. J. Phys. Oceanogr., 29, 1314–1333.

Kubokawa, A., and T. Inui, 1999: Subtropical countercurrent in an idealized ocean GCM. J. Phys. Oceanogr., 29, 1303–1313.

Macdonald, A. M., T. Suga, and R. G. Curry, 2000: An isopycnally averaged North Pacific climatology. J. Atmos. Oceanic Technol., in press.

Nitani, H., 1972: Beginning of the Kuroshio. In Kuroshio – Its Physical Aspects, Univ. of Tokyo Press, pp. 129–163.

Suga, T., and K. Hanawa, 1995: The subtropical mode water circulation in the North Pacific. J. Phys. Oceanogr., 25, 958–970.

Suga, T., Y. Takei, and K. Hanawa, 1997: Thermostad distribution in the North Pacific subtropical gyre: The central mode water and the subtropical mode water. J. Phys. Oceanogr., 27, 140–152.

Takeuchi, K., 1984: Numerical study of the subtropical front and the subtropical countercurrent. J. Oceanogr. Soc. Japan, 40, 371–381.

Uda, M., and K. Hasunuma, 1969: The eastward subtropical countercurrent in the western North Pacific Ocean. J. Oceanogr. Soc. Japan, 25, 201–210.

Yoshida, K., and T. Kidokoro, 1967: A subtropical countercurrent (II) – A prediction of eastward flows at lower subtropical latitudes. J. Oceanogr. Soc. Japan, 23, 231–246.

Interannual variability of natural and anthropogenic carbon and transient tracers in the Labrador Sea, 1993–2000

Kumiko Azetsu-Scott, E. Peter Jones and Igor Yashayaev, Department of Fisheries and Oceans, Bedford Institute of Oceanography, Canada; and Robert M. Gershey, BDR Research Limited, Canada. Azetsu-ScottK@mar.dfo-mpo.gc.ca

Deep convection in the Labrador Sea in late winter produces a relatively homogeneous water mass, Labrador Sea Water (LSW). This well-ventilated water mass, characterised by low salinity and temperature, is an important vehicle for the transport of atmospheric gases, including carbon dioxide and transient tracers such as chlorofluorocarbons (CFCs), to intermediate depths of the North Atlantic Ocean. At depth, North East Atlantic Deep Water (NEADW) and Denmark Strait Overflow Water (DSOW) flow into the region. Therefore, all of the water masses that are primarily responsible for thermohaline circulation in the North Atlantic can be observed in the Labrador Sea.

The Labrador Sea is a highly dynamic region. The salinity and temperature of LSW, as well as the depth to which the water mass is ventilated in the winter, has varied significantly over the last five decades. Minima in temperature and salinity were observed in mid 50s, 70s and most recently in the 1993–1994 winter with deep convection to a depth of about 2200 m. Variable lateral mixing of slope water also modifies LSW. These variations influence the sequestration and transport processes of anthropogenic gases. Further, carbon dioxide sequestration is influenced by surface biological processes. Inorganic carbon and transient tracers (CFC-11, CFC-12, CFC-113 and CCl_4) have been measured annually since 1993 along WOCE AR7W section in the Labrador Sea (Fig. 1). We describe the spatial and interannual variability of natural and anthropogenic carbon and CFCs (only CFC-12 is shown in this article) during the increasing salinity and temperature phase in LSW (1300–1900 m). This study is a part of ongoing efforts to identify the processes that control air-sea exchange and fate of anthropogenic CO_2 in the North Atlantic.

Anthropogenic CO_2 was calculated using the method of Brewer (1978), Chen and Millero (1979) and Gruber (1996) as follows:

$$CT_{ant} = CT_{measured} - CT_{bio} - CT_{280} - CT_{dis}$$

Here CT_{ant} and $CT_{measured}$ are the concentrations of anthropogenic and measured total inorganic carbon respectively. CT_{bio} is the change of total inorganic carbon caused by biological processes, namely photosynthesis, respiration and formation and dissolution of $CaCO_3$. CT_{280} is the total inorganic carbon concentration at equilibrium with a pre-industrial atmosphere ($fCO_2 = 280\ \mu$atm). CT_{dis} is the air-sea disequilibrium of CO_2 at the time of water formation. The analytical precision of the total inorganic carbon measurements, $CT_{measured}$, was $\pm 2 - 3\ \mu$mol / kg. The overall uncertainty in CT_{ant} is estimated at $\pm 7\ \mu$mol / kg at best. The analytical precision of the CFC-12 measurement is in the range of 1–3%. The method was described in detail by Tait et al. (2000).

In the central Labrador Sea, three water masses are clearly identified by CT_{ant} and CFC-12 distributions (only CFC-12 distribution is shown in Fig. 2, page 18). NEADW has its core around 2800 m. It is characterised by a salinity maximum and low concentrations of CT_{ant} and CFC-12 as

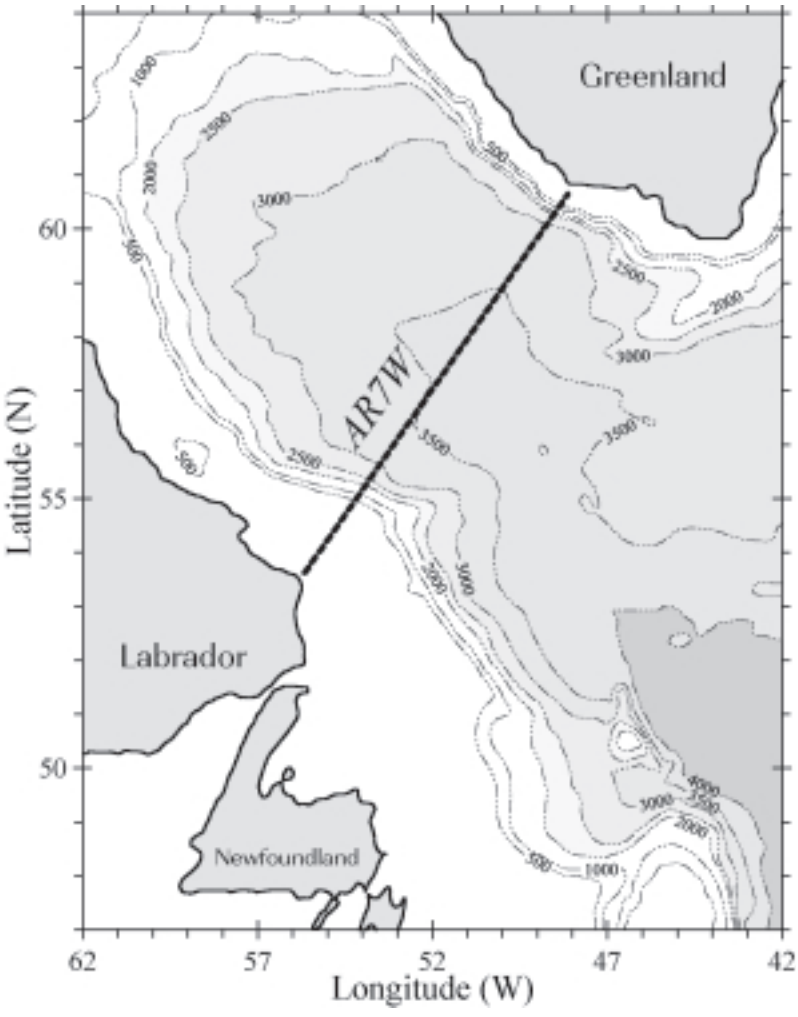

Figure 1. Location of WOCE AR7W line in the Labrador Sea.

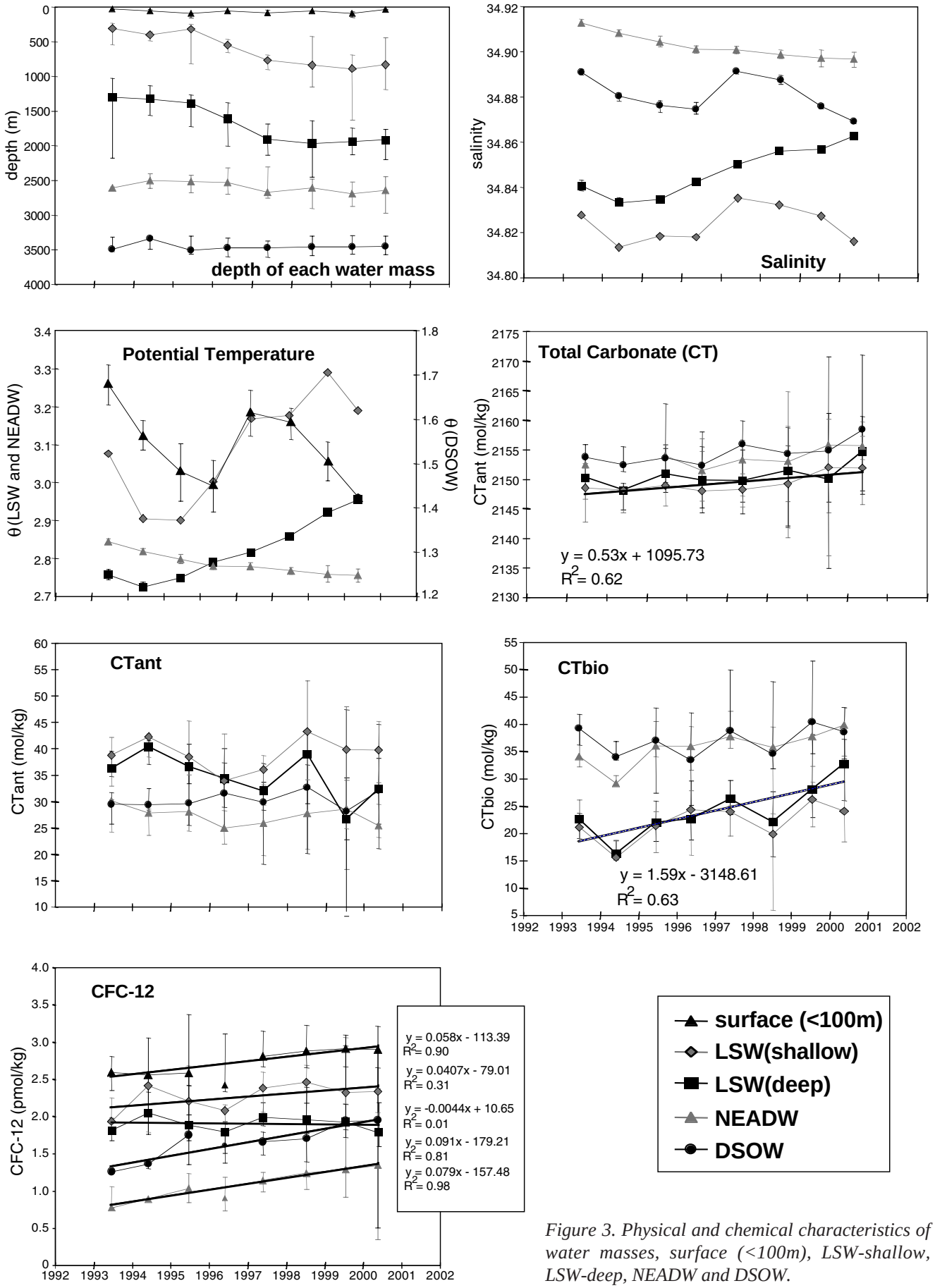

Figure 3. Physical and chemical characteristics of water masses, surface (<100m), LSW-shallow, LSW-deep, NEADW and DSOW.

a result of its relatively old ventilation age (10–15 years) compared to the underlying DSOW (6–9 years) (Tait et al., 2000). DSOW is found in general at depths >3500 m in the central Labrador Sea and is characterised by lower salinity and higher concentrations of CT_{ant} and CFC-12 than those found in NEADW. LSW is locally formed and fills the upper 2200 m of the central Labrador Sea. LSW shows higher CT_{ant} and CFC-12 concentrations than those in the underlying waters. The high concentration of CFC-12 on the Labrador Shelf corresponds with cold and fresher water transported by the Labrador Current. On both the east and west sides of the basin, relatively low concentrations of CFC-12 are observed at the depths around 1500 m. CFC-12 distributions demonstrate well-defined deep convection plumes, which showed higher concentrations of CFC-12 in the central Labrador Sea in 1995 and 1999 and on the eastside of the Labrador Sea in 1998. Lateral mixing of slope water and core LSW was also observed. In general, CFC-12 levels increased during the period of study. This is especially most pronounced in upper 1000 m. NEADW and DSOW also showed an increase of concentrations of CFC-12 with time.

The chemical and physical properties of each water mass were calculated, using samples taken from the Central Labrador Sea, where the topographic depth exceeds 3300 m (from 300 km to 750 km in the horizontal range in Fig. 2). North East Atlantic Deep Water (NEADW) was defined as $36.965 < \sigma_2 < 37.000$ and Denmark Strait Overflow Water (DSOW) occupies the 200 m off the bottom. Labrador Sea Water (LSW) was divided into 3 layers, surface (<100 m), shallow LSW (LSW-shallow) and deep LSW (LSW-deep). LSW-deep was defined from T-S diagram as a region of minimum salinity and temperature each year (Yashayaev et al., 2000). LSW-shallow occupies the region between 100 m deep to the top of LSW-deep. Averages of each water mass at each station were calculated for salinity, θ, $CT_{measured}$, CT_{ant}, CT_{bio} and CFC-12. Medians among stations are shown in Fig. 3 with maximum and minimum values as vertical lines for the depths of each water mass and chemical measurements and median absolute deviation for salinity and temperature.

The depth of LSW-deep has increased since 1993. Salinity and temperature profiles show that a homogeneous water mass was developed by intensive convection to a depth of 2200 m in 1993–1994. The temperature and salinity of LSW-deep have increased since 1994. During this period, the convection depth did not exceed 1200 m. By contrast, the salinity and temperature of NEADW decreased during this period. This trend in salinity and temperature is similar to that of LSW-shallow. The total carbonate concentration (CT) in the ocean is subject initially to the surface water and the atmospheric conditions during the air-sea interaction and subsequent alteration after carbon was transferred to the ocean from atmosphere. The former includes the carbon dioxide concentration in the atmosphere and salinity, temperature, alkalinity and partial pressure of carbon dioxide in the surface water. The latter includes biological processes, primary production, respiration and formation and dissolution of calcium carbonate, and mixing of water masses with different carbonate concentrations. During the period of study, an increase of CT was observed only in LSW-shallow. CT concentration increased with depth in all years except 1999. The concentration of CT_{ant} is highly variable both in space and time, partly because of the method used to estimate CT_{ant}, which includes multiple variables and assumptions. However, the resolution of water masses is demonstrated, with younger water having higher concentrations of CT_{ant}, i.e., LSW-shallow>LSW-deep>DSOW>NEADW. A significant increase in CT_{bio} with time was observed only in LSW-deep. Concentrations of CFC-12 increased in the near surface layer (<100 m), NEADW and in DSOW. The increase was especially evident in very surface water. In LSW-deep, CFC-12 did not show any increase over the time of this study. When considered along with the increase of CT_{bio} in the same layer, this can be taken as an indication that LSW-deep was produced during the deep convection year of 1993–1994 and has been trapped in this region since then. The concentration of CFC-12 is at the same level both in LSW-deep and DSOW in 1999, suggesting that both water masses were last exposed to the atmosphere at the same time. Since the age of DSOW is 6–9 years, when it arrived at the Labrador Sea, this is additional evidence that LSW-deep has been trapped since the last deep convection of 1993–1994. Since the range of variation of salinity and temperature during this study has little influence on the solubility of CO_2 and CFCs, their seawater concentrations are primarily the result of the atmospheric mixing ratios of these gases.

In summary, profiles of anthropogenic CO_2 and CFC-12 demonstrated the three principal water masses in the central Labrador Sea. The concentrations of these tracers decrease in correspondence with the ages of water masses, LSW-shallow>LSW-deep>DSOW>NEADW. Average CT_{ant} concentrations in each water mass are 39, 35, 30 and 27 μmol / kg, respectively. However, due to the uncertainties and assumptions used in the calculation of anthropogenic CO_2, the method is not robust enough to resolve the interannual variation that is evident in the CFC-12 measurements. Weakening of convection in the central Labrador Sea after the intensive convection event of 1993–1994 left the water mass, LSW-deep, in the depth range 1500–2200 m. In LSW-deep, salinity and temperature increased slightly along with the increase of CT_{bio}, while CFC-12 concentration did not change, indicating this water mass was trapped and ageing. In contrast to LSW-deep, the surface water of the Labrador Sea, DSOW and NEADW all demonstrate increased concentrations of CFC-12, reflecting the consistent annual exposure of these water masses to the atmosphere. The combination of CFC-12 and the biological component of carbonate concentration provides a tool for understanding the behaviour of these water masses.

Acknowledgement

We are grateful to scientists of Bedford Institute of Oceanography and the officers and crew of the CSS Hudson,

who conducted the lengthy cruises over the years. Our special thanks go to Pierre Clement, Frank Zemlyak, Mike Hingston and Anthony Isenor. Val Tait paved the road for this work. This work was supported by PERD.

References

Brewer, P. G., 1978: Direct observation of the oceanic CO_2 increase. Geophys. Res. Lett., 5, 997–1000.

Chen, C.-T. A., and Millero, F. J., 1979: Gradual increase of oceanic CO_2. Nature, 205–206.

Gruber, N., 1998: Anthropogenic CO_2 in the Atlantic Ocean. Global Biogeochemical Cycles, 12, 165–191.

Tait, V. K., R. M. Gershey, and E. P. Jones, 2000: Inorganic carbon in the Labrador Sea: Estimation of the anthropogenic component. Deep-Sea Res., 47, 295–308.

Yashayaev, I. M., R. A. Clarke, and J. R. N. Lazier, 2000: Recent decline of the Labrador Sea Water. International Council for the Exploration of the Sea (ICES), CM, 2000/L, p18.

Inconsistency in the conductivity of the standard KCl solution made from the different high-quality chemicals

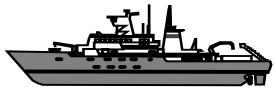

Takeshi Kawano, Japan Marine Science and Technology Center, Yokosuka; Michio Aoyama, Meteorological Research Institute, Tsukuba, Japan; and Yasushi Takatsuka, JAMSTEC. kawanot@mailgate.jamstec.go.jp

Aoyama et al., (1998) (A98 hereafter) propose the "offset" table of IAPSO Standard Seawater (SSW) batches P103–P129. They show that the salinity differences at the WHP crossover points in the Pacific are much improved when the "offset table" is applied. They used the batches P123 and P124 as key batches to match up the experimental results made by various institutions during the period from 1991 to 1997 under the assumption that the SSW does not change so much during this period. Their hypothesis is that the batch to batch differences reported by various studies such as Mantyla (1994), Takatsuki et al. (1991), A98 and so on are, to a considerable extent, the reflection of the "initial offset". On the other hand, Ridout and Culkin (1998) and Culkin and Ridout (1998) claim that the label salinity is correct when it was produced. They argue that the offset measured in such a manner as A98 may be incorrect when applied to salinity data retrospectively since the most of the change in the conductivity in the SSW is thought to occur as a result of so-called "ageing effect". Bacon et al. (1998) show, as an example of "ageing effect", that the difference from label salinity of SSW batch P128 was 0.0015–0.0020 when it was 25 months old although it was 0.0001 in A98. They assert that the simple correction of SSW like A98 will not be appropriate and conclude that the crucial factor in assessing inter-cruise salinity difference from the point of view of SSW is the age of SSW at the time of usage. In their article, they guessed that the measurement of A98 was made close to the time of production, however, this is not correct. The measurement of A98 was made in May 1997, actually. SSW batch P128 was 22 months old at time of the measurement. The difference between A98 and Bacon et al. (1998) was caused by the difference of the "reference". Bacon et al. (1998) assumed that the SSW batch P132 is "correct". According to our recent result, the "offset" of P132 is calculated to be -1.7×10^{-3} in salinity with the same reference as A98. When we assume P132 is correct,

Table 1. The result of comparison among reproducible standard KCl solutions made from different companies and batches. ΔZ_{15} is Z_{15} observed minus Z_{15} calculated.

Year	Chemicals	Z_{15} calculated	Z_{15} observed	ΔZ_{15}
1999	Company A	0.999985	1.000042	0.000057
		0.999998	0.999669	-0.000329*
		0.999995	1.000047	0.000052
		1.000077	1.000144	0.000067
		1.000145	1.000200	0.000055
	Company B	1.000255	1.000221	-0.000035
2000	Company A	1.001339	1.001406	0.000066
		0.997082	0.997148	0.000066
	Company C	1.001718	1.001799	0.000080*
		1.000155	1.000283	0.000127
		0.999801	0.999920	0.000119
	Merck 1	0.999340	0.999353	0.000013
		1.002587	1.002615	0.000028
		1.015670	1.015686	0.000016
	Merck 2	0.997741	0.997781	0.000040
		0.998981	0.999052	0.000071
		1.001345	1.001401	0.000055
		0.999726	0.999787	0.000060
		0.999597	0.999649	0.000052
		1.000221	1.000272	0.000051
	Merck 3	1.000507	1.000614	0.000106
		0.998642	0.998776	0.000134
		1.000031	1.000093	0.000062*

P128 was 1.8×10^{-3} salty at the time of measurement and this is coincident with the result of Bacon et al. (1998).

The "offset" in A98 should be considered as a relative value to the mean of batch-to-batch difference of SSW P91–P102. It does not necessarily mean directly the absolute difference between label salinity and "true" salinity. As mentioned by Ridout and Culkin (1998), the only way to check the change in SSW is to make measurement against the standard KCl solution (UNESCO, 1981), freshly prepared. Accordingly, we prepare the standard KCl solution from the high-quality chemicals (99.999% purity) of four companies including Merck "Suprapur", which was used by Dauphinee et al. (1980) (D80 hereafter) in UNESCO background papers.

Method

The measurement was made in May 1999 and June 2000. In 1999, we prepared the standard KCl solution from the KCl made by Company A and B. In 2000, we prepared the standard KCl solution from the Company A, Company C and three different batches of Merck. The method of preparation is almost same as D80. We used a pure water filtered by a MILLIPORE Milli-Q SP whose conductivity was more than 18 mMHO cm. We dried KCl at 500°C for 12 hours. The conductivity was measured by Guildline Autosal 8400B using SSW batch P132 as a tentative reference. The method of the measurement is written in Aoyama et al. (submitted). The temperature of the bath of the Autosal was measured by Hewlett-Packard model 2804A quartz thermometer (HP2804A), which is calibrated periodically. The bath temperature of the Autosal was set to 24°C and the actual temperature measured by HP2804A was 24.000 ±0.001°C. We employ the equation (2a) and (3) in D80 to evaluate the measurements.

Results and discussion

Table 1 shows a result of our experiment. Note that the observed Z_{15} is a value referred to the SSW batch P132 and 3×10^{-5} in Z_{15} is equivalent to 0.001 in salinity. "Z_{15} calculated" is the value calculated from equation (2a) in D80, "Z_{15} observed" is the value calculated from equation (3) in D80 and means "Z_{15} observed" minus "Z_{15} calculated". Except for some bad measurements ("*"in the table), reproducibility of the four solutions made from the same KCl was quite well. For example, the standard deviation (1σ) of 4 solutions made from Company A is about 1.2×10^{-5} in Z_{15} and 1σ of 6 solutions of Merck 2 is about 1.1×10^{-5} in Z_{15}. The scattering of the measured value is the same extent as seen in D80.

Although chemical companies certify the purity of 99.999%, the major problem during the weighting is likely to be water remained along with KCl powder/beads. In order to check the magnitude, the residual water after drying was measured by Karl-Fisher Method. We selected 3 batches of Merck "Suprapur" and one batch of Company C. As the result of 19 measurements (ca. five samples from each batches), the residual water after drying was 13.3 ±3 ppm. This residual water is corresponding to

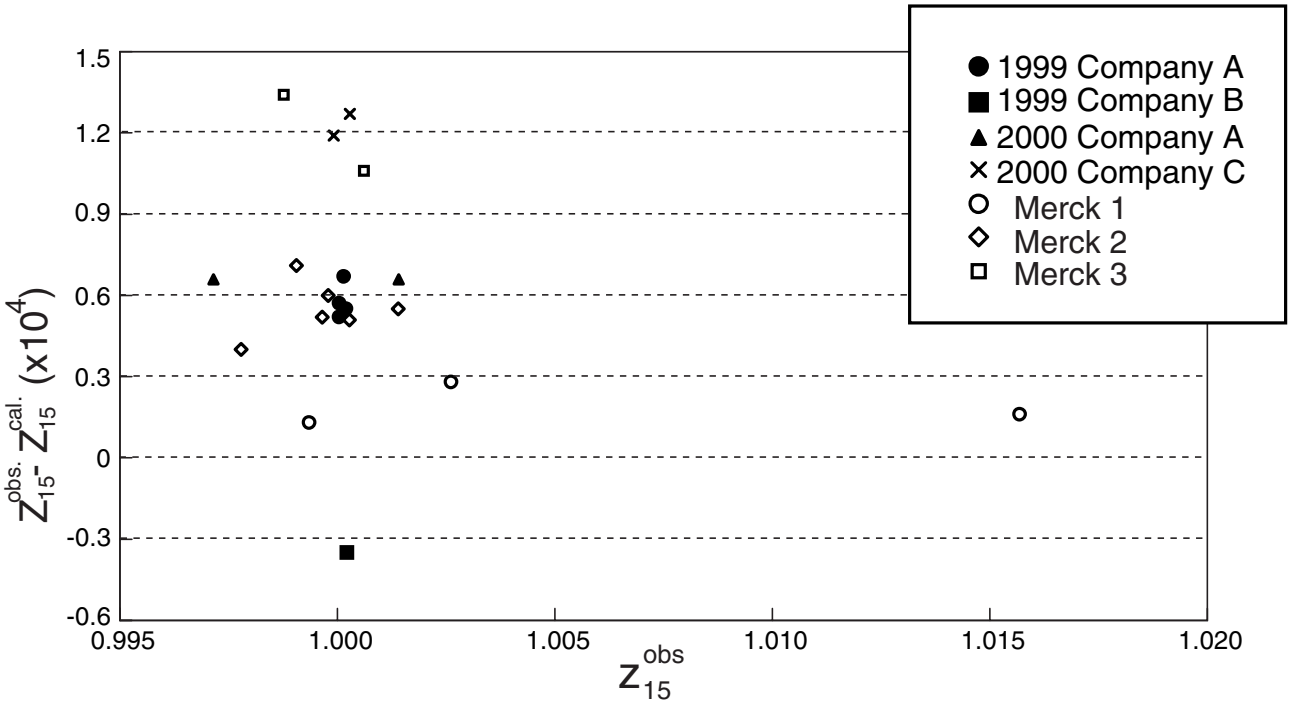

Figure 1. The result of comparison among reproducible standard KCl solutions made from different companies and batches. X axis is Z_{15} observed and Y axis is Z_{15} observed minus Z_{15} calculated. The values put "" in Table 1 are not plotted in this figure. Note that 0.3×10^{-4} in Z_{15} is equivalent to 0.001 in salinity.*

about 0.0003 in salinity. This uncertainty of 0.0003 in salinity is the same order of the magnitude of the uncertainty originated from the solution prepared 99.999% purity KCl. The effect of residual water, however, could be negligible in our comparison experiment because residual water were almost same in each samples.

Fig. 1 also shows the result of our experiment. The values put "*" in Table 1 are not plotted in this figure. A company dependency and a batch dependency in the same company are obviously seen in this Figure. We can find the same sort of the batch dependency in the Table III of Poisson (1980). Poisson (1980) measured the resistance of "Fused KCl solutions" and calculated their concentration corresponding to the resistance of SSW of 35‰ at 15°C. According to the result, the concentration of Merck Flask B was 32.4361 ±0.0004 g/Kg, while the concentration of Merck Flask C was 32.4354 ±0.0002 g/Kg. This difference is corresponding to 0.2×10^{-4} in Z_{15} and also corresponding to 0.8×10^{-3} in salinity. In our experiment, the difference between Merck 1 and Merck 3 is 0.8×10^{-3} in Z_{15}, which is equivalent to about 0.003 in salinity. This result suggests that the company dependency and/or batch dependency in the same company may possibly be the cause of "initial offset". Therefore, the batch-to-batch differences in the "offset table" are the sum of "initial offset" due to the batch dependency of KCl solution and possible "ageing effect". We are preparing a more detailed paper on the standard KCl solutions and the most recent SSWs. What we would like to emphasise is that essentially some kind of new definition of salinity and practically some new method to keep the traceability of the SSW might be required.

References

Aoyama, M., T. Joyce, T. Kawano, and Y. Takatsuki: Standard Seawater comparison up to P129. Submitted.

Aoyama, M., T. Joyce, T. Kawano, and Y. Takatsuki, 1998: Offset of the IAPSO Standard Seawater through the batch P129 and its application to Pacific WHP crossovers. Int. WOCE Newsl., 32, 5–7.

Bacon, S., H. Snaith, and M. Yelland, 1998: An example of Ageing in IAPSO Standard Seawater. Int. WOCE Newsl., 33, 25–26.

Culkin, F., and P. S. Ridout, 1998: Stability of IAPSO Standard Seawater. J. Atmos. Oceanic Technol., 15, 1072–1075.

Dauphinee, T. M., J. Ancsin, H. P. Klen, and M. J. Phillips, 1980: The effect of concentration and temperature on the conductivity ratio of potassium chloride solutions to Standard Seawater of Salinity 35‰ (Cl 19.3749‰). IEEE J. Oceanic Eng., OE-5, No. 1, 17–21.

Guildline Instruments Ltd., 1991: Service Manual for Model 8400B "Autosal". Guildline Instruments Ltd.

Mantyla, A. W., 1994: The treatment of inconsistencies in Atlantic deep water salinity. Deep-Sea Res., 41, 1387–1405.

Poisson, A., 1980: The concentration of the KCl solution whose conductivity is that of Standard Seawater (35‰) at 15ºC. IEEE J. Oceanic Eng., OE-5, No. 1, 24–28.

Ridout, P. S., and Culkin, 1998: Offsets of IAPSO Standard Seawater. Int. WOCE Newsl., 33, 20.

Takatsuki, Y., M. Aoyama, T. Nakano, H. Miyagi, T. Ishihara, and T. Tsutsumida, 1991: Standard Seawater comparisons of some recent batches. J. Atmos. Oceanic Technol., 8, 895–897.

UNESCO, 1981: Tenth report of the Joint Panel on Oceanographic Tables and Standards. UNESCO Tech. Paper in Mar. Sci., 36, 25pp.

Comments on Kawano et al., 'Inconsistency in the conductivity of the standard KCl …'

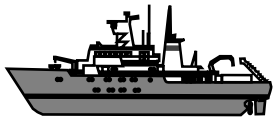

F. Culkin and P. S. Ridout, IAPSO Standard Seawater Service, Ocean Scientific International Ltd., UK. paul.ridout@oceanscientific.co.uk

This paper raises some important points about the calibration of Standard Seawater and we welcome this opportunity to comment on the findings and to set out our reasons for disagreeing with them.

When the Practical Salinity Scale 1978 (PSS-78) was formulated, the conductivity of a KCl solution containing 32.4356 g/kg (corrected for buoyancy) was adopted as the reference standard for salinity determinations. It was agreed, in advance by the Joint Panel on Oceanographic Tables and Standards, that Merck "Suprapur" KCl, suitably dried, would be used for the KCl reference solution. This salt has excellent purity, a well-referenced chemical analysis (Dauphinee, 1980; Perkin and Lewis, 1980; Poisson, 1980) and no differences were found between batches (Dauphinee et al., 1980). The purity of the water used to prepare the KCl solutions was not defined or specified. However, the three laboratories (in Canada, England and France), which carried out the basic work of establishing the defined KCl concentration obtained excellent agreement, suggesting that the waters purified by double distillation or deionisation were of comparable quality.

In accordance with the recommendations of PSS-78, the Standard Seawater Service has always used high purity KCl supplied by Merck, initially brand-named Suprapur and later, in the UK, Aristar. The manufacturers assure us that these two brands are identical in specification and that there is no difference between batches. We have certainly not seen any differences in switching from one batch to another. We would suggest that if there were differences between batches as great as Kawano et al. report, then we

at the Standard Seawater Service or the users of Standard Seawater would have noticed.

To provide more evidence of the consistency of Merck KCl, we recently carried out a direct comparison between two batches of Aristar KCl by determining K_{15} for a bottled seawater. The standard method of calibrating Standard Seawater, as described in Culkin, 1986 was used. Basically this consists of preparing 5 solutions of KCl, covering the concentration range 32.3–32.6 g/kg, measuring their conductivities on a Guildline Autosal salinometer previously calibrated with IAPSO Standard Seawater, and interpolating the conductivity, at 15.000°C, corresponding to a concentration of 32.4356 g/kg. This procedure was carried out using 2 different batches of Aristar KCl and the results are shown in Table 1.

Table 1

KCl Batch	KCl Conc.	R-21 Meas.	R-15 Calc.	Cond. ≡ 32.4356 g/kg	K-15 of Bottled Seawater
B 734739 622	32.262 52	0.986 53 5	0.994 96 3	1.00001 2	0.999 91
	32.301 36	0.987 62	0.996 05 2		
	32.450 58	0.991 97 5	1.000 45 0		
	32.303 92	0.987 76	0.996 19 9		
B 544439 020	32.728 59	0.999 74	1.008 28 1	1.00000 7	0.999 91
	32.519 20	0.994 02 5	1.002 51 7		
	32.427 40	0.991 31	0.999 77 9		
	32.432 98	0.991 47 5	0.999 94 5		
	32.342 56	0.988 83	0.997 27 8		

These results show clearly that no differences were detected between these two batches though, admittedly, they do not rule out differences between the three batches examined by Kawano et al. We do think, however, that more credibility would be given to their findings if they were to clarify the following points.

1. The Standard Seawater Service measures the conductivity of 5 KCl solutions to produce a straight line relationship from which to interpolate the conductivity at the defined concentration (i.e. the result is the mean of 5 sets of weighings and conductivity measurements). Kawano et al. rely on only one, which is surely less reliable. This conclusion is borne out by their findings that Delta-Z varies between 0.000 04 and 0.000 07 for Merck 2 and between 0.000 06 and 0.000 13 for Merck 3 and the range is even greater for the Company A product. Even omitting the extreme results, which the authors do without explanation or justification, these results do not inspire much confidence in the methodology. We would suggest using the procedure that has been used by the Standard Seawater Service for many years.
2. The accuracy of the conductivity measurements depends crucially on the initial calibration of the

salinometer with Standard Seawater. The authors say that P132 was used as a "tentative" reference, but, by the time (June 2000) the Merck measurements were carried out, P132 was three years old. We would recommend that the authors check their P132 against a more recent batch of Standard Seawater because their high KCl results could be interpreted as being due to a small change in P132 on storage.

3. A minor point, but did the authors use a temperature on IPTS-68 or ITS-90?

With the present tendency to demand an extra decimal place in salinity determinations and the dependence on a reliable source of high purity KCl, the authors may well have a point in suggesting that a new definition of salinity is required, but it is far from clear how to improve on the present one.

References

Culkin, F., 1986: Calibration of Standard Seawater in electrical conductivity. The Science of the Total Environment, 49, 1–7.

Dauphinee, T. M., 1980: Introduction to the Special Issue on the Practical Salinity Scale 1978. IEEE J. Oceanic Eng., OE-5(1), 1.

Dauphinee, T. M., J. Ancsin, H. P. Klein, and M. J. Phillips, 1980: The effect of concentration and temperature on the conductivity ratio of potassium chloride solutions to Standard Seawater of salinity 35 ppt (Cl 19.3740). Introduction to the Special Issue on the Practical Salinity Scale 1978. IEEE J. Oceanic Eng., OE-5(1), 17.

Perkin, R. G., and E. L. Lewis, 1980: The Practical Salinity Scale 1978: Fitting the Data. IEEE J. Oceanic Eng., OE-5, (1), 6.

Poisson, A., 1980: The concentration of the KCl Solution whose conductivity is that of Standard Seawater (35ppt) at 15°C. IEEE J. Oceanic Eng.,OE-5,(1), 25.

WOCE/CLIVAR Representativeness and Variability Workshop, 17–20 October 2000, Fukuoka, Japan

Contributed by members of the Science Organising Committee

The collection of data in the WHP will define a benchmark for the state of the ocean during WOCE. However, here is one important issue; how typical may this benchmark be, compared to the historical data? And to what degree are the WHP data "synoptic"? Or put another way, to what extent did the ocean substantially change DURING the WOCE sampling? How consistent are the various WOCE data sets with one another and how well can models (that assimilate or not) "represent" the data? These questions illustrate the issue of representativeness, one important aspect of WOCE Goal 2.

Another aspect of WOCE Goal 2 is to develop understanding of variability so that better climate models and observations can be combined in the future. This is squarely in the domain of the Climate Variability and Predictability Study (CLIVAR), which seeks to understand interannual, decadal and longer periods of climate variability. Scientific hypotheses continue to develop about the different roles of the atmosphere and ocean in climate variability. These will guide what process experiments will be needed and what sustained measurement systems of the future will look like. As far as the ocean is concerned, our understanding of the variability as measured in WOCE and its potential sources is critical for progress on defining both CLIVAR and the Global Ocean Observing System (GOOS) envisioned to provide sustained observations of the ocean in the decades ahead.

Thus we see the need to use WOCE to look backward and forward in time, and have configured this workshop with some specific goals, which are as follows:

- To review information gained on seasonal to interannual variability during WOCE,
- To assess information gained on decadal variability from comparison of WOCE and pre-WOCE data,
- To estimate the impact of this variability on the representativeness of the WOCE (particularly WHP) data sets and derived quantities (e.g. heat and freshwater fluxes),
- To review the ability of models to represent seasonal and longer-term ocean variability and the variation in water mass properties, volumes and formation rates,
- To identify, and take steps to initiate, data analysis and modelling research needed to better assess the representativeness of WOCE data sets and derived quantities,
- To identify the principal mechanisms (e.g. local or remote air–sea exchange, advection, propagation, coupled air–sea processes) behind the oceanic signals of climate variability as measured in WOCE, and
- To make recommendations based on the workshop conclusions for the design of future research (CLIVAR) and operational (GOOS) observing systems.

In total, there were 65 posters presented and a total number of registered attendees of 81. The workshop consisted of plenary sessions with one or two keynote speakers. After the talks, all of the posters in a given session were briefly introduced and the workshop then shifted to the poster session room. Because of the more than adequate space for posters, it was possible for all posters from all sessions to be up and in place for the entire workshop. Various special focus topics were suggested by the Science Organising Committee and these evolved into six special sessions. The final plenary session was a summary of all of

the various formal and informal sessions, with a discussion of the major results presented and issues discussed. Below, a brief summary is presented for each of the Sessions and Focus Discussions.

Global views of WOCE variability: data and models

The principal speakers in this session were Sergei Gulev (air–sea fluxes) and Dudley Chelton (satellite altimetry). As advertised, the session presented a global perspective of the following: surface fluxes, satellite observations, ocean observations, ocean models, coupled models and ocean state estimation. There was a clear demonstration that in integrating the surface heat fluxes from VOS measurements to give implied northward heat transports, the uncertainties grow far too much for the calculation to be of much use. However, over much of the North Atlantic for example, the uncertainties (e.g. sampling) are not too large for the implied divergence of the ocean heat transport to be useful in constraining direct estimates from ocean sections. The converse is also true.

Combining satellite scatterometer winds with microwave SSTs revealed regions of enhanced wind stress and curl associated with oceanic fronts, with implications to frontal dynamics and biological production in such regions. The NSCAT and QuikSCAT data have allowed quantitative assessment of the accuracy of the wind field analyses produced by the ECMWF and NCEP operational weather forecast models. The results show a significant improvement in ECMWF between the October 1996–June 1997 period of the NSCAT data record and the August 1999–present period of the QuikSCAT data record. The most significant improvement has been in the tropics, but the accuracy of the operational analyses of 10 m winds has also improved significantly at middle and high latitudes. It should be noted, however, that the spatial resolution of the operational analyses are still limited to scales longer than approximately 500–700 km. As a consequence, ECMWF and NCEP considerably underestimate the intensities of the derivative wind fields (divergence and curl).

The results shown in the session display variability almost everywhere and in nearly every quantity observed during WOCE. In particular, the 8-year TOPEX data record has detected energetic variability on time scales from monthly to interannual and space scales from 100 km to global. On seasonal, interannual and even decadal time scales the variability matches that observed in the atmosphere. Of particular importance here are the repeat XBT lines. Ocean models, both hindcasts and coupled to an atmosphere, are being used to extend this ocean variability in time and space, and to investigate mechanisms for its generation and propagation.

Principal mechanisms for variability

The principal speakers in this session were Jim Hurrell and Kimio Hanawa. Hurrell spoke about the state of the atmosphere during WOCE. It is expected that much of the

Participants in the photograph are (from left to right): in the sixth (back) row: Sokov, Komori, Uchida, I. Kaneko, Miyamoto, Stammer, Park, Sprintall, Goda, Kashima; in the fifth row: Yang, Toyoshima, S. Aoki, Nakamura, Dinh, Shimizu, Awaji, Zhu, Ishikawa, Gulev, Hurrell, Chapman, Umatani, Fukasawa; in the fourth row: Hatayama, Kitamura, Suga, Peter, Aoyama, Josey, Ito, Uehara, Böning, Killworth, Dewar, D.-K. Lee, H.-J. Lie; in the third row (right-hand-side two-thirds): Naveira-Garabato, A. Kaneko, Proshutinsky, Alexiou, Wakata, Hishida, Sugimoto, Takeuchi; in the second row: Ichikawa, Matsuo, Otoki, Gould, Holliday, Hanawa, Nagata, Swift, Azetsu-Scott, Banks, Lumpkin, Y. Aoki, Tokmakian, Boscolo, Cunningham; and in the first (front) row: Haak, Cornuelle, Beal, Lotfi, le Traon, Webb, Imawaki, Joyce, Roemmich, Koltermann, Large, Bindoff, Chelton, Kubota.

oceanic variability is forced by the atmosphere. The WOCE period was characterised by pronounced deviations from the long term mean conditions in both the Northern and Southern Hemispheres. In the North Pacific, North Atlantic and Southern Oceans there were low atmospheric pressure anomalies at high latitudes and high anomalies at low latitudes, resulting in stronger than average westerlies. This behaviour produced unprecedented high values of the North Atlantic Oscillation index (NAO) and low values of the North Pacific Index (NPI).

Hanawa presented evidence that fluctuations in the NPI and the Kuroshio properties were 90° out of phase and suggested that this was indirect evidence of a coupled oceanic/atmospheric process involving the two phenomena. Bill Dewar's poster examined an analytic/QG model of a coupled interaction at mid-latitudes of this process and again suggested that this may be part of a coupled mode between the atmosphere and the ocean. This issue was re-visited in the focus group discussion later (see below).

Other new results presented in this session included:

- an illustration of how oceanic shear affects the speed of propagation of oceanic anomalies (Killworth)
- an example of how Ekman pumping can generate high frequency variability of the barotropic modes of the ocean (Webb)
- the role of Kelvin and Rossby waves in connecting Pacific and Indian Ocean variability via the Indonesian Passages (Yang)
- the use of WOCE hydrography in the study of the changes in the thermohaline flows in the Atlantic to the NAO (Dobroliubov)
- the importance in eddy fluxes in affecting the structure of the meridional overturning circulation in the tropics, with the eddies being responsible for O(10%) of the total heat flux (Danabasoglu).

Model/data comparisons: where are we?

The session had one invited presentation (D. Stammer) and eight posters. In his invited presentation, D. Stammer presented results on model and data comparison at high frequencies and at the mesoscale. He showed that models have now significantly improved and can be used to help data interpretation. He then focused his presentation on data assimilation and efforts underway to derive a consistent, global 4-D description of the ocean state. First assimilation results at low resolution are encouraging. The optimisation is working and, in particular, heat flux errors appear to be corrected in the right way to reduce the misfit between data and models. The current work deals with the comparison of the outputs of the assimilation system with WOCE data. A future (GODAE) plan is to improve the model resolution and physics.

One of the main lessons from this session (and from posters in other sessions) is that unconstrained models do show skills in reproducing some variability signals. They can thus be used to better explore these variability signals. Many illustrations of this joint use of data and models have been presented in the workshop. The next and complementary step will be to merge the data and models through data assimilation.

Pacific/Indian variability

Various topics were discussed. The oral presentation by Dean Roemmich addressed the upper ocean variability. Mainly the basin-wide meridional transport and its relatively quick adjustment to wind stress changes and the interannual variability of net meridional heat transport. Its mean value at mid-latitude of North Pacific is 0.8 PW, which is close to the estimate from surface heat flux derived from ECMWF fields.

The contributions from the posters are summarised as follows:

Pacific Ocean

- Estimation of the western boundary current of the North Pacific subarctic gyre flow field and its transport from the combination of in situ observation and altimetry data.
- The Kuroshio transport south of Japan shows small seasonal variability, the observed decadal variability of the transport compares well with the Sverdrup transport with some delay.
- Climatological mean temperature sections of upper ocean obtained from VOS high-density XBT network for the North and South Pacific.
- Bottom water in the North Pacific is warming. This results from a study of one-time repeat hydrography from 1985 to 1999.
- Decadal variability of Ekman pumping velocity, as derived from sea-level pressure field for the last 100 years, shows a climatic regime shifts in 1940s and 1970s.

Indian Ocean

- Mass and heat transports across the equator due to the seasonal and intraseasonal variation of wind stress were presented.
- The seasonal signal is found to penetrate down to the 3,000 m depth in the flow field.
- Study of decadal change of deep water masses shows that temperature and salinity in the main thermocline (on a neutral density surface) at 20°S decreased from 1960s to 1980s.

Southern Ocean and Arctic variability

This session had two invited talks and 11 posters. The main focus areas for this session was transport variations of the Antarctic Circumpolar Current, the Antarctic Circumpolar Wave, short-term changes and decadal changes in water masses of Southern Ocean Origin and in the Arctic Region.

A new method for estimating the transport anomalies on WOCE SR3 section between Tasmania and Antarctica was presented in the talk by Bindoff. This method, based on the correlation obtained from CTD data between steric sea-level height and depth integrated steric anomaly, was used to show the rapidly changing transport variation that were observed south of Australia. The rapidity of the transport variations (weeks time-scales) showed how important it is to monitor transport variation time-scales. Striking water mass changes in bottom waters on both short time scales, and longer time-scales in Drake Passage was also shown. Drake Passage AABW and Scotia Sea AABW show considerable changes in position between repeated hydrographic sections, only a few years apart. The changes in the Scotia Sea are thought to be related to changes in the path of AABW from the Weddell Sea through the Scotia Island chain. On longer time-scales comparison of hydrographic data in the Indian, Pacific and Atlantic Ocean have all shown that SAMW and AAIW have changed. A coherent pattern of freshening of AAIW (suggesting a freshening of surface waters) and a cooling and freshening of density surfaces of SAMW is consistent with a warming of this water mass. South of the SAF only the near-surface waters (below the T min layer) and above the salinity maximum show significant difference in water mass characteristics. The exact reason for this is not clear but could be an increased transport of UCDW across the ACC. In the Arctic Region quite distinct changes have been observed in the ocean circulation, sea-level pressure (the Arctic trough is now deeper), precipitation (has increased) and temperature (now warmer) over the last 100 years according to the oral presentation by Andrey Proshutinsky. The changes in the Arctic region seem to parallel the changes in the Southern Ocean over the last 30 years (circumpolar trough is now deeper, suggesting stronger westerlies) and from re-analysis runs (by NCEP) suggesting increased rainfall.

Atlantic variability

John Gould's overview, with material provided by Bob Dickson, highlighted the extremely variable character of the Atlantic on all time-scales and the nature of this variability. He also summarised the findings of last year's North Atlantic Workshop in Kiel. As the main conduit between both poles this ocean shows strong and rapid changes induced via the deep, intermediate and deep waters at high latitudes. During WOCE the role of several elements of this rapid adjustment process have become clear: the importance of deep convection to the formation of intermediate water masses, the rapid delivery of newly-formed intermediate waters from high latitudes by boundary currents to moderate latitudes, and that the full-depth circulation of the North Atlantic, and its meridional heat transports, are closely linked to large-scale changes in atmospheric forcing, namely the North Atlantic Oscillation. The coupled ocean–atmosphere system of the Atlantic Ocean has marked and obvious effects on its bordering continents, and also ties into the global variability pattern, as shown for the most recent ENSO event.

Most prominent was the reaction of the North Atlantic circulation to the dramatic drop in the NAO index from its all-time high in the winter of 1995/6 and the as dramatic recovery. Although definitely not adequate for a coverage of decadal changes, the WOCE data set here captured a significant and so far unremarked large-scale event in both atmosphere and ocean.

In all, eight posters covered various aspects of the Atlantic Ocean variability, including changes in the deep hydrographic constituents and water masses, in boundary current transports and ocean-wide transports of heat and freshwater. Exchanges processes with the Arctic Ocean and the European North Polar Mediterranean Seas have also been described. Several modelling experiments show promising insights into the physics underlying these changes, and indicate that modellers and observationalists finally may start talking the same language.

The group discussions had the following foci:

- Representativeness: Seasonal/Interannual Variability (chair D. Roemmich)
  What was learned about seasonal-to-interannual (SI) variability of the oceans during WOCE?
  What are the implications for the interpretation of limited duration WOCE datasets (e.g. WHP one-time, current meter arrays, floats,…)?
- Representativeness: Decadal Variability in WOCE (chairs P. Koltermann and N. Bindoff)
  The value of WOCE experiment for Decadal Time scales
  Decadal differences are pervasive
  Decadal differences observed during the WOCE period need to be monitored
  Need to focus on mechanisms of decadal changes
  What should future programmes include that are not currently in WOCE?
  Resolution of seasonal cycle
- Towards better surface flux estimates (chair W. Large)
  Wind velocity/stress:
  Precipitation:
  Radiation:
  Turbulent fluxes
- Variability Hypotheses (chair D. Webb)
  Internal Oceanic Variability
  Variability driven by the Atmosphere
  Coupled Variability
  Other interactions
- Model/data Comparisons and Assimilation (chair P.-Y. le Traon)
  Consistency between data and models for the different variability signals (intraseasonal, seasonal, inter-annual, decadal) – where are we?
  What should be done in the future as far as model/data comparisons are concerned?
  Data assimilation and WOCE/CLIVAR: what are the needs and how do we assess the value of a data assimilation system?
- Future Observations (chair D. Roemmich)
  Given the background (OceanObs99,…) plus the experience of WOCE, what is the present status of

planning and what modifications and additional planning are needed for ocean observations in CLIVAR etc.?
What is needed to move from the planning phase to carrying out the observations?

Workshop conclusion

WOCE was not designed fundamentally to address the issue of "Variability". However, much was learned during WOCE and this new knowledge will guide the design of future climate studies (CLIVAR) and observational systems (GOOS). It is likely that many of the scientific questions addressed but not answered by this workshop, will find their way into CLIVAR/GOOS workshops of the future.

Sponsors

Japan Science and Technology Corporation, Japan
World Climate Research Programme
Science and Technology Agency, Japan

Science Organising Committee

Terry Joyce, Chair, Woods Hole Oceanographic Institution, Woods Hole, USA
Shiro Imawaki, Co-chair, Kyushu University, Kasuga, Japan
Nathan Bindoff, University of Tasmania, Hobart, Australia;
Kimio Hanawa, Tohoku University, Sendai, Japan
Peter Koltermann, Bundesamt für Seeschiffahrt und Hydrographie, Hamburg, Germany
Bill Large, National Center for Atmospheric Research, Boulder, USA
Pierre-Yves le Traon, CLS, Ramonville Saint-Agne, France
Dean Roemmich, Scripps Institution of Oceanography, La Jolla, USA
David Webb, Southampton Oceanography Centre, Southampton, UK

Local Organising Committee

Shiro Imawaki, Chair, Kyushu University, Kasuga, Japan
Kaoru Ichikawa, Secretary, Kyushu University, Kasuga, Japan
Kimio Hanawa, Tohoku University, Sendai, Japan
Takeshi Matsuno, Kyushu University, Kasuga, Japan
Yutaka Nagata, Marine Information Research Center, Japan
Maki Otoki, Japan Science and Technology Corporation, Kawaguchi, Japan
Nobuo Suginohara, University of Tokyo, Tokyo, Japan
Kiyoshi Takahashi, Kyushu University, Kasuga, Japan
Hiroshi Uchida, Japan Science and Technology Corporation, Kawaguchi, Japan
Shin-ichiro Umatani, Kyushu University, Kasuga, Japan
Tetsuo Yanagi, Kyushu University, Kasuga, Japan

MEETING TIMETABLE 2001

January 8–12	Decadal Climate Variability Workshop	Hawaii, USA
January 14–19	Climate Variability, the Oceans and Social Impact (AMS)	Albuquerque, USA
January 22–25	CLIVAR Pacific Implementation Panel	Hawaii, USA
February 12–15	GODAE Steering Group Meeting	Noumea, New Caledonia
March 5–6	WG on Ocean Model Development	Santa Fe, USA
March 19–23	23rd WCRP JSC Meeting	Boulder, USA
March 25–30	EGS XXVI General Assembly	Nice, France
May 14–18	CLIVAR SSG 10th Session	Toulouse, France
May 21–25	WCRP/SCOR Workshop on Intercomparison and Validation of Ocean–Atmosphere Flux Fields	Washington, DC, USA
May 29–2 June	AGU 2001 Spring Meeting	Boston, USA
June 25–29	WOCE Ocean Transport Workshop	Southampton, UK
July 10–13	IGBP Open Science Conference	Amsterdam, NL
August 20–24	Climate Conference 2001	Utrecht, NL
October 8–13	Conference on the Oceanography of the Ross Sea	Ischia-Naples, Italy
October 21–28	IAPSO-IABO 2001: an Ocean Odyssey	Mar del Plata, Argentina
December 10–14	AGU 2001 Fall Meeting	San Francisco, USA

The WOCE International Newsletter is published by the WOCE International Project Office.

Editor:
Roberta Boscolo

Compilation and layout:
Sheelagh Collyer

The International WOCE Newsletter is distributed free-of-charge upon request thanks to the funding contributions from France, Japan, UK, and WCRP.

This Newsletter provides a means of rapid reporting of work in progress related to the Goals of WOCE as described in the WOCE Scientific and Implementation Plan.

Requests to be added to the mailing list and changes of address should be sent to:
WOCE IPO
Southampton Oceanography Centre
Empress Dock
Southampton SO14 3ZH
United Kingdom
Tel. +44 23 8059 6205
Fax. +44 23 8059 6204
e-mail: woceipo@soc.soton.ac.uk

Contents of past issues together with the electronic PDF version can be found at:
http://www.soc.soton.ac.uk/OTHERS/woceipo/acrobat.html

Articles, letters, announcements and reviews are welcome and should be addressed to the editor.

Printed by Technart Ltd.
Southern Road
Southampton SO15 1HG
United Kingdom.

If undelivered please return to:

WOCE IPO
Southampton Oceanography Centre
Empress Dock
Southampton SO14 3ZH
United Kingdom.

CONTENTS OF THIS ISSUE